Simulation of rare events in the experiments at underground

Realistic simulated events has same features of real data :
Digital output of many electronics channels

Full chain of simulation : Generator, matter particle interactions, signal propagation, electronics and digitisation

Ideal vs real detector simulation

- **Why do we need an underground laboratories ?**
- **Underground facilities around the world**
- **Simulation of BOREXINO experiments [Astroparticle Physics 97 (2018) 136, Phys. Rev. D89 (2014) 112007]**
- **Simulation of ICAL detector [Pramana 88 (2017) 55]**
- **Conclusion**

Cosmic muon interactions and particles at the earth atmosphere

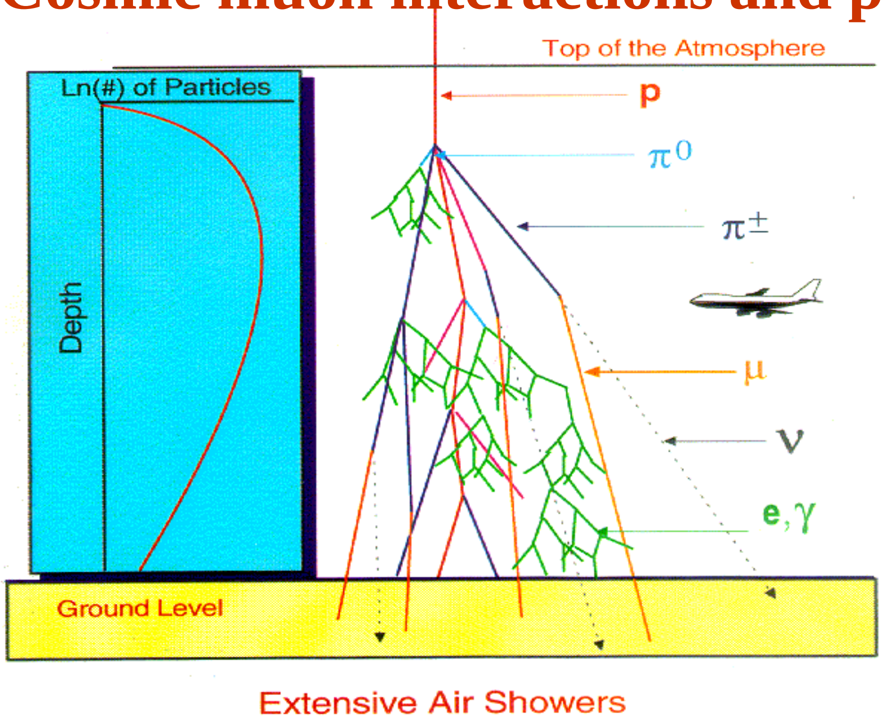

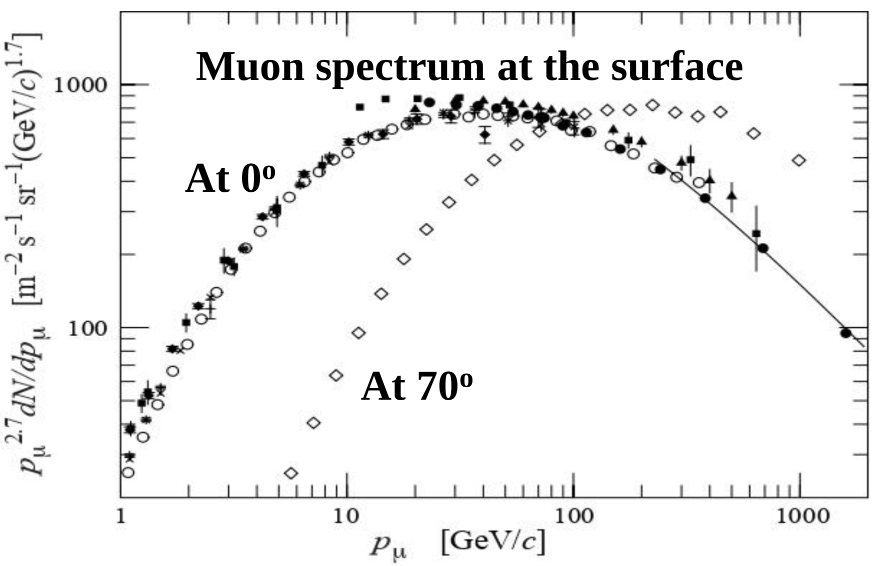

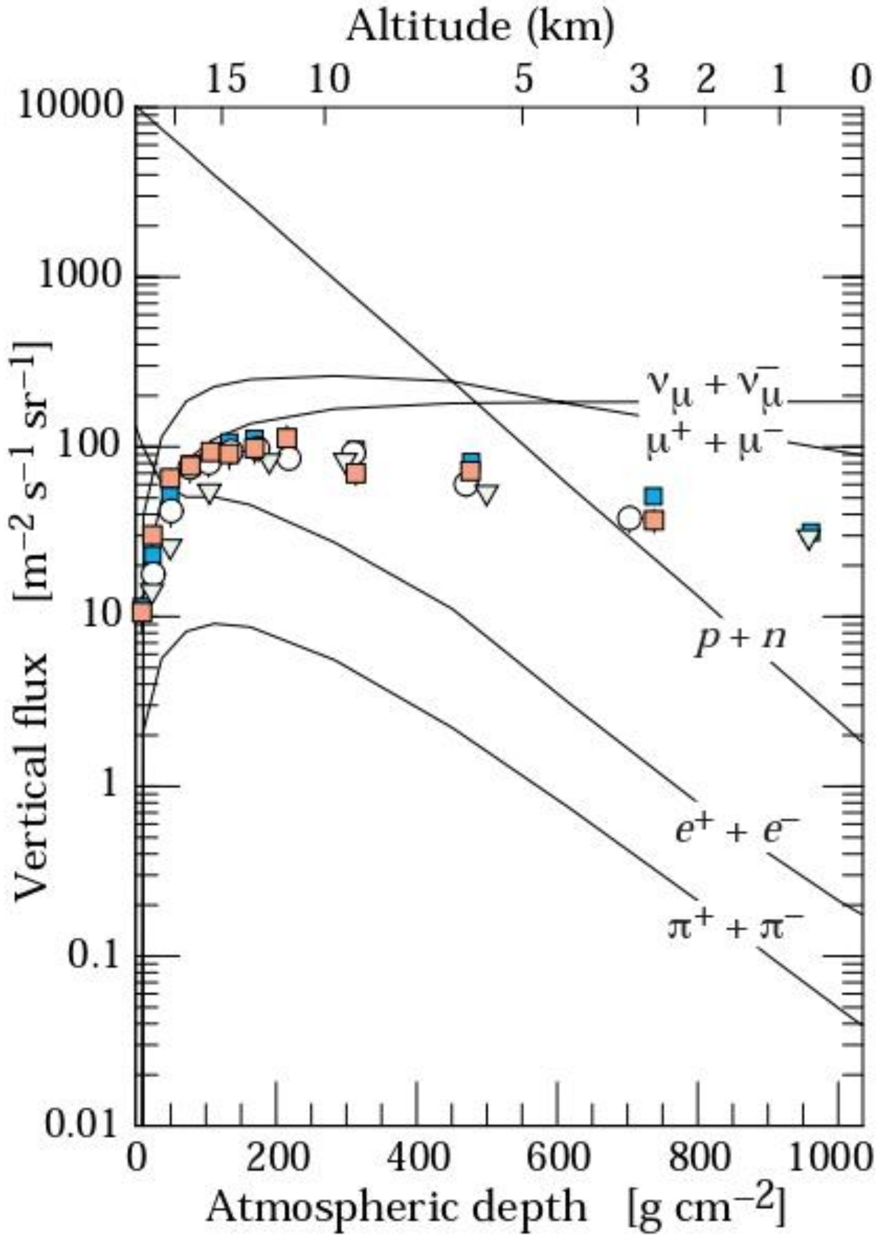

Muon and Muon Induced Neutron production

The rate of the atmospheric neutrino interactions is about 200 kt^{-1} $year^{-1}$.
Rate at the surface due to cosmic ray particles is very frequent, namely ~200 m^{-2} s^{-1},

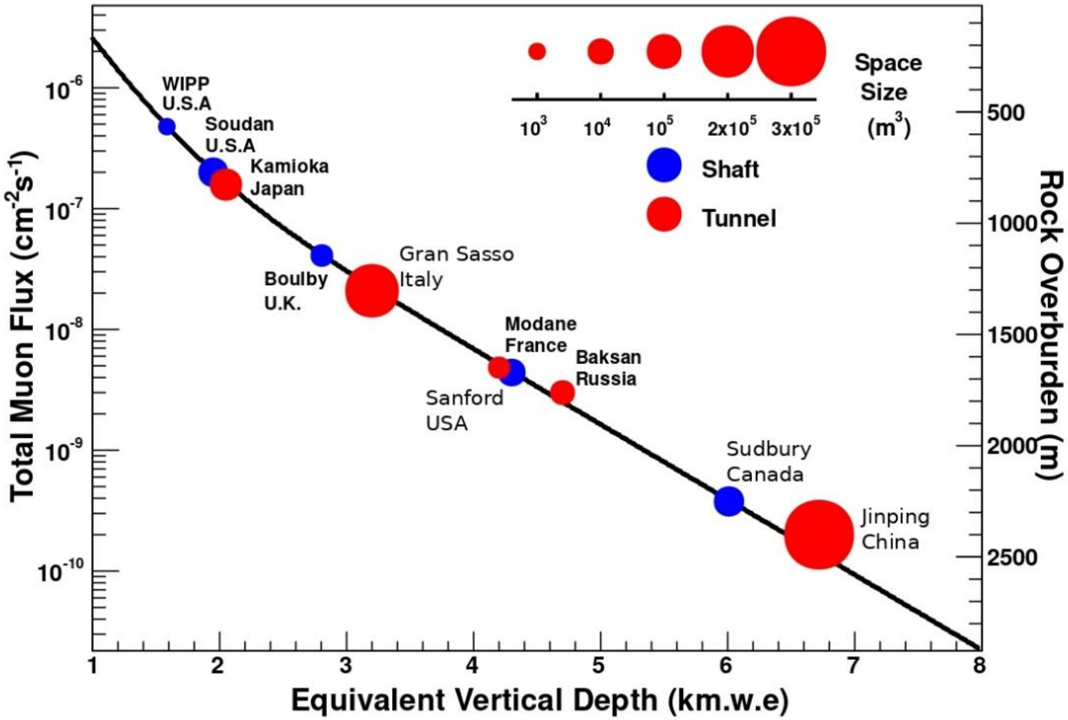

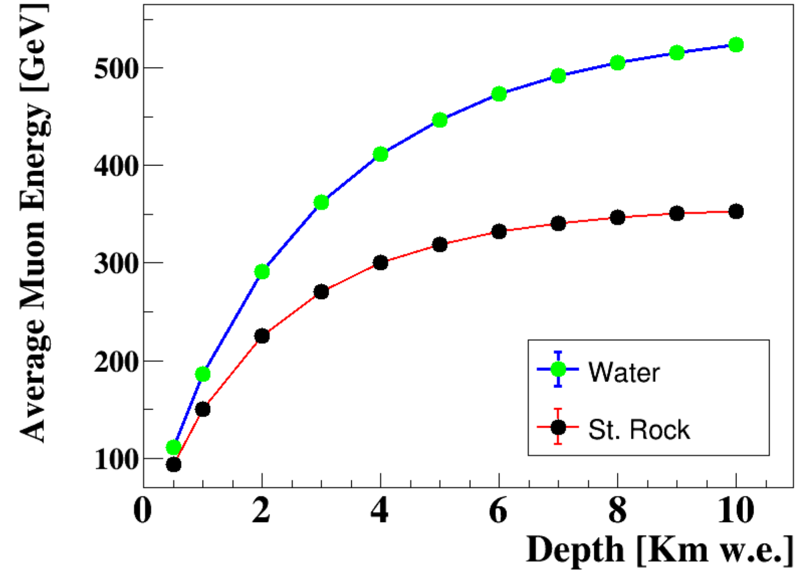

Non only muon, particles produced in muon interaction are more important

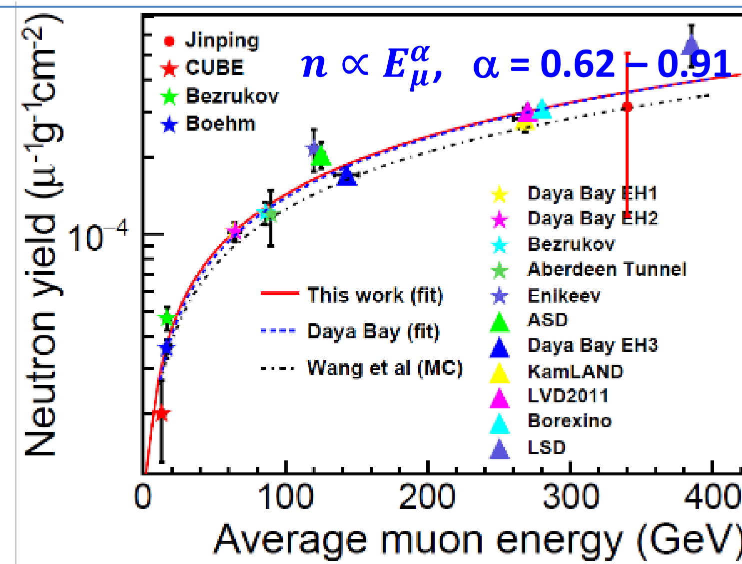

Deepest experimental halls :

EPR Mine in South Africa : 8800 m.w.e

KGF : Deepest : 8400m.w.e (whereas neutrino discovery at 7500m.w.e)

Cosmogenic isotopes in Borexino

Residual rate after 300ms time veto after each muon pass through ID

Isotope	Lifetime	Energy [MeV]	Decay	Residual rate
n	255μs	2.23	Capture γ on ^{1}H	< 0.005
^{12}N	15.9ms	17.3	β^+	$< 5\times10^{-5}$
^{13}B	25.0ms	13.4	$\beta^-\gamma$	$< 5\times10^{-5}$
^{12}B	29.1ms	13.4	β^-	$(7.1\pm0.2)\times10^{-5}$
^{8}He	171.7ms	10.7	$\beta^-\gamma n$	0.004±0.002
^{9}C	182.5ms	16.5	β^+	0.020±0.006
^{9}Li	257.2ms	13.6	$\beta^-\gamma n$	0.022±0.002
^{8}B	1.11s	18.0	$\beta^+\alpha$	0.210±0.050
^{6}He	1.16s	3.51	β^-	0.310±0.040
^{8}Li	1.21s	16.0	$\beta^-\alpha$	0.310±0.040
^{11}Be	19.9s	11.5	β^-	0.034±0.006
^{10}C	27.8s	3.65	$\beta^+\gamma$	0.540±0.040
^{7}Be	76.9days	0.478	EC γ	0.360±0.050

Underground Facilities : Present and future

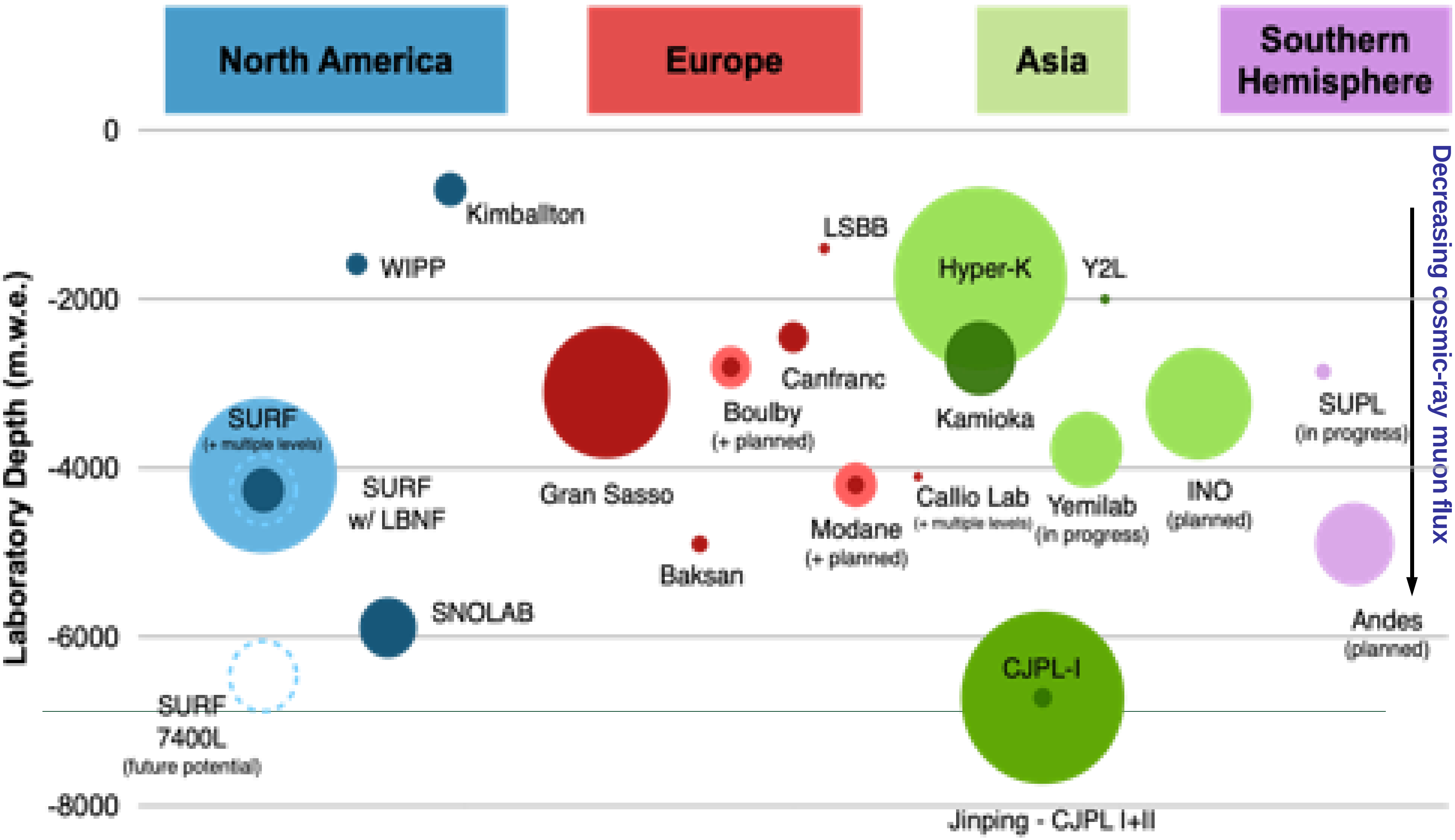

Gran Sasso Deep Underground Laboratory

- Running
- Construction/Commissioning
- Decommissioning

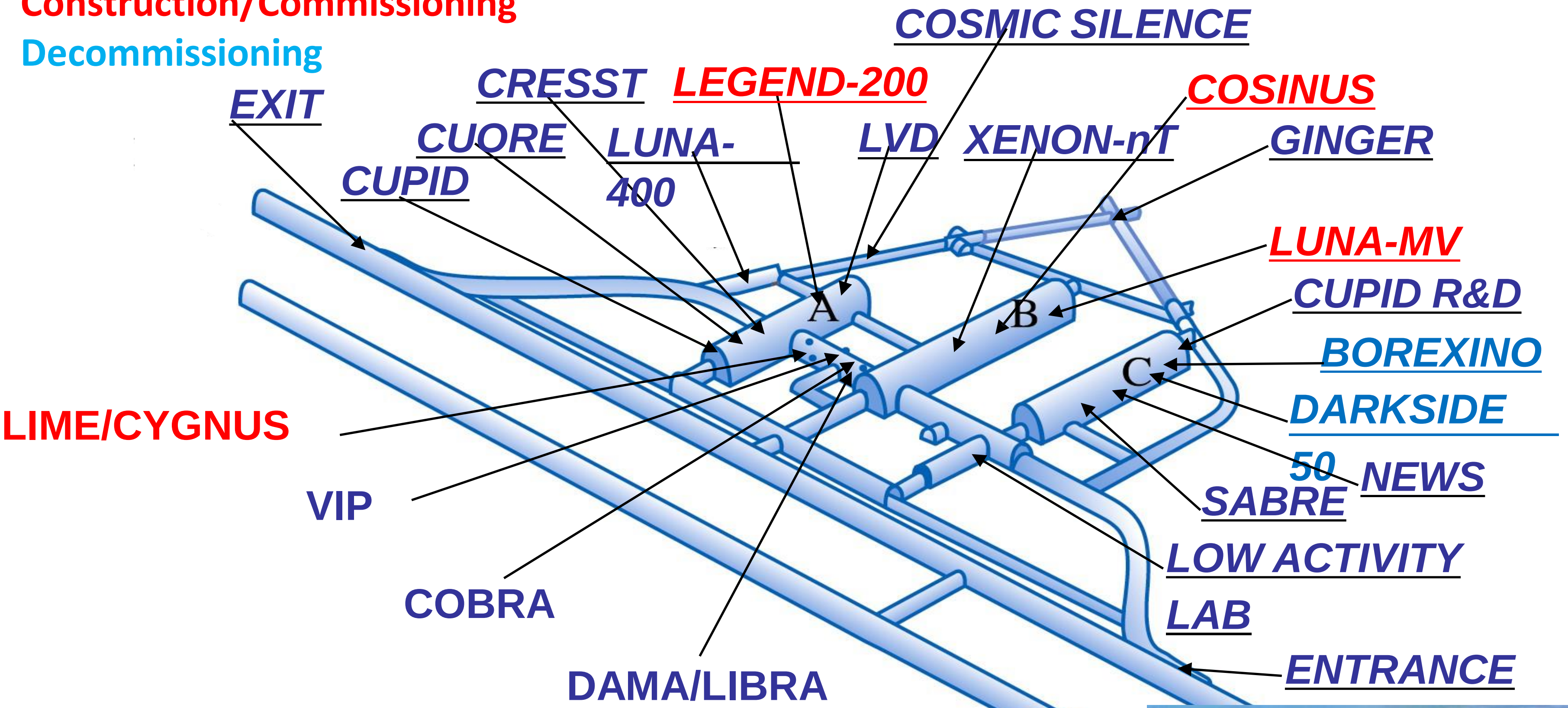

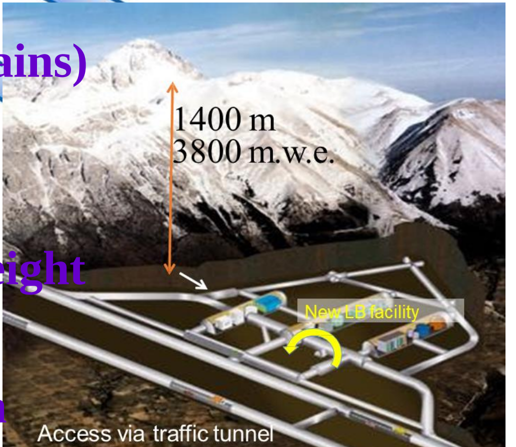

- Shielded by 1400 m (3800 m.w.e .) of rock (Gran Sasso Mountains)
- Total Muon flux 3×10^{-8} cm^{-2} s^{-1} (reduction factor ~10^6)
- Easy access directly from the A24 highway
- 3 main experimental halls 100 m long, 20 m width and 18 m height
- Many small tunnels for lab facilities and small experiments
- There are 20 experiments in data taking or under construction

Different experiments at LNGS

(Laboratori Nazionali del Gran Sasso)

- **Dark matter : CRESST, XENON-nT, COCINUS, DARKSIDE, SARBE (NaI), DAMA/LIBRA, LIME/CYGNUS**
- **NDBD : CUPID, CUORE, COBRA, LEGEND, COBRA**
- **Nuclear Astrophysics : LUNA**
- **Neutrino : LVD, BOREXINO** : BORon solar neutrino Experiment : (From Italian name, like CERN)
- **COSMIC SILENCE : "On the potential adaptive role of environmental background radiation"**
- **GINGER : Fifth force ?**
- **VIP : Violation of the Pauli Exclusion Principle**

Borexino Detector

- Steel water tank (WT) of 9m bas radius and 16.9m height filled with ~1kt ultrapure water
  - 208 8” PMT on floor and outer surface of a SS sphere, 6.85m radius
- The inner detector within SSS equipped with
  - 2212 8” PMT (from 1931 in Dec 2007 to 1183 in April 2019) : Photocathode coverage : 34%
  - Three ID layers with insertion of two 125μm think nylon balloons. Inner vessel (IV) and outer vessel (OV) with radii 4.25 and 5.50m
  - The two layers between the SSS and the IV, separated by the OV, form the outer buffer (OB) and the inner buffer (IB).
- Liquid scintillator
  - Pseudocumene (PC, 1,24-trimethylbenzene, $C_6H_3(CH_3)_3$)
  - Fluorescent dye PPO (2,5-diphenyloxazole, $C_{15}H_{11}NO$), 1.5g/l
  - Density : $(0.878 \pm 0.004)\ \mathrm{gcm}^{-3}$
  - Target mass : 278 ton
  - Proton density : $(6.007 \pm 0.001) \times 10^{28}\ \mathrm{ton}^{-1}$
- Buffer consisting soln of the dimethylphthalate, DMP, $C_6H_4(COOCH_3)_2$) light quencher in PC

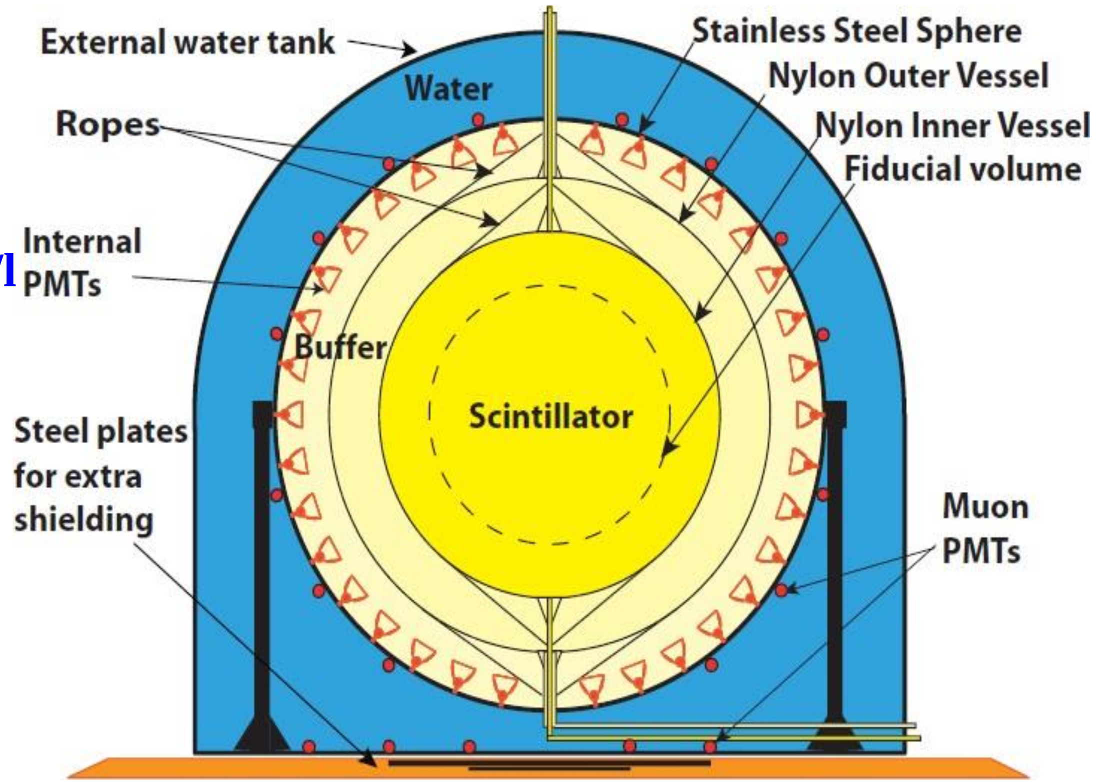

BORXINO detector components

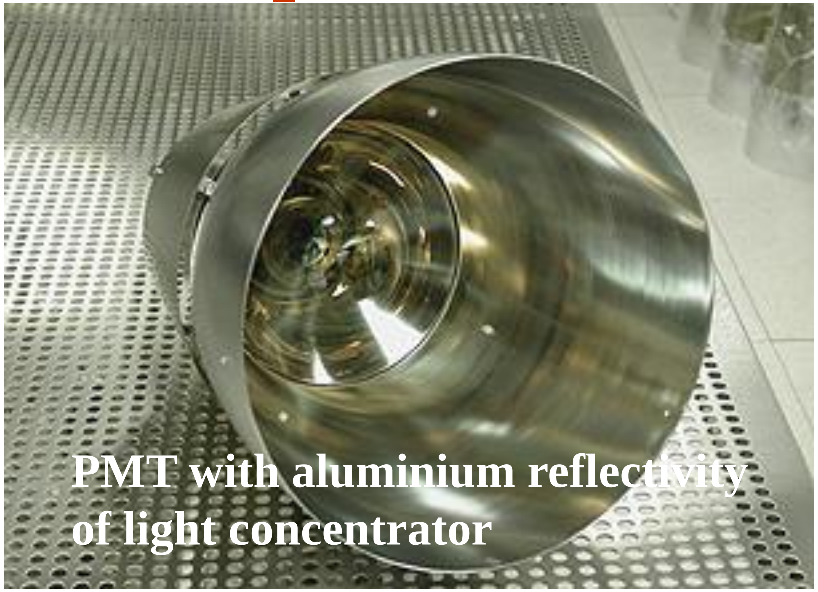

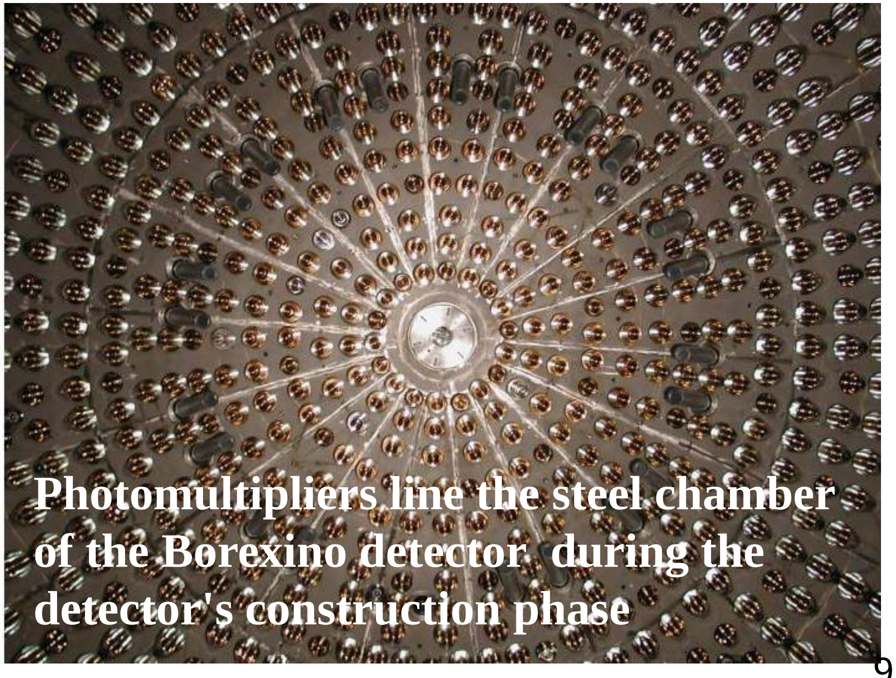

The fully-assembled Borexino detector is visible from multiple cameras embedded in the structure.

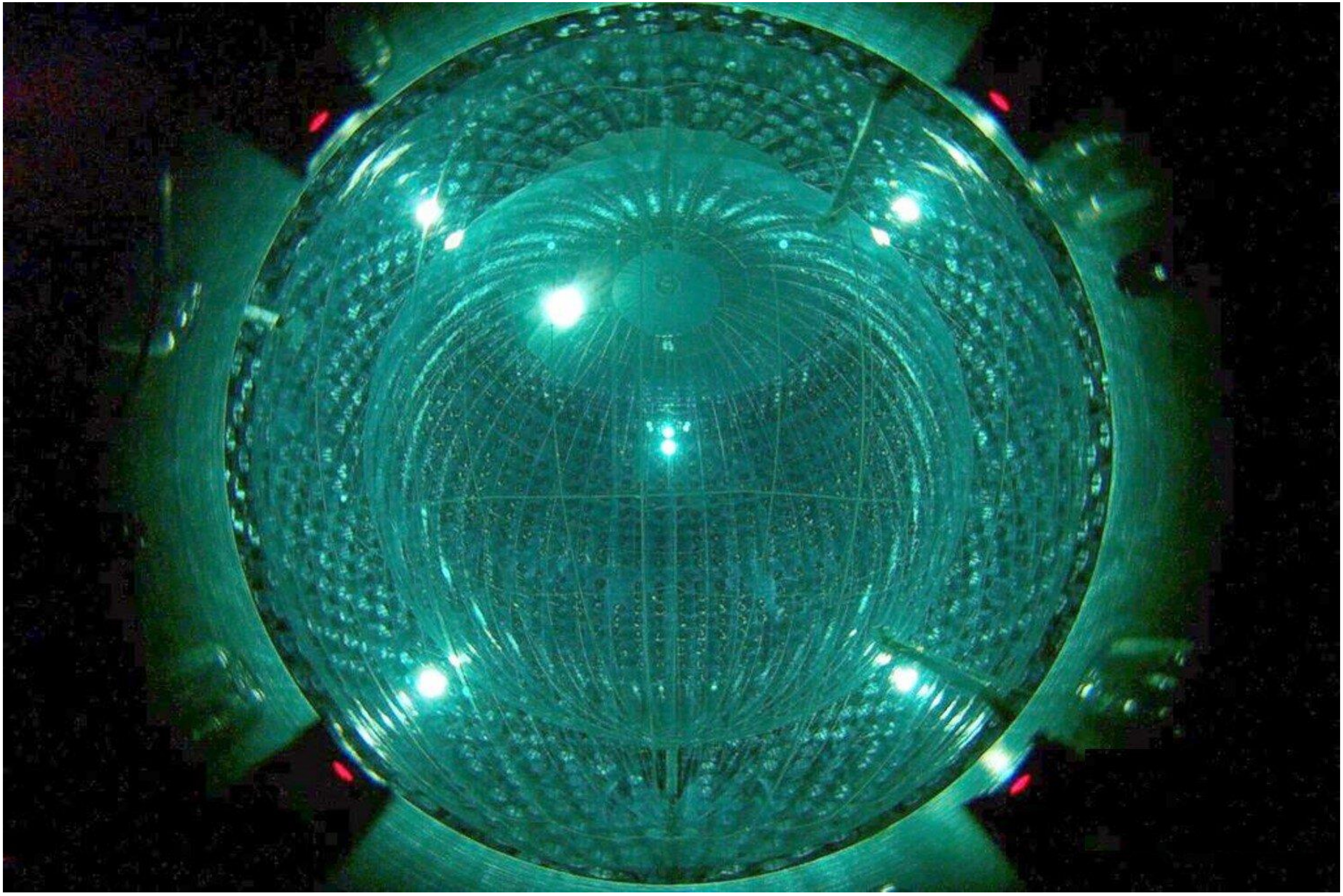

Solar Neutrino

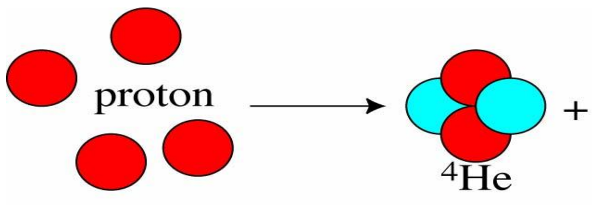

$2e^+ + 2\nu_e + 25\text{MeV}$

$L_{sun} \sim 4 \times 10^{26}$ W

2×10^{38} ν/sec

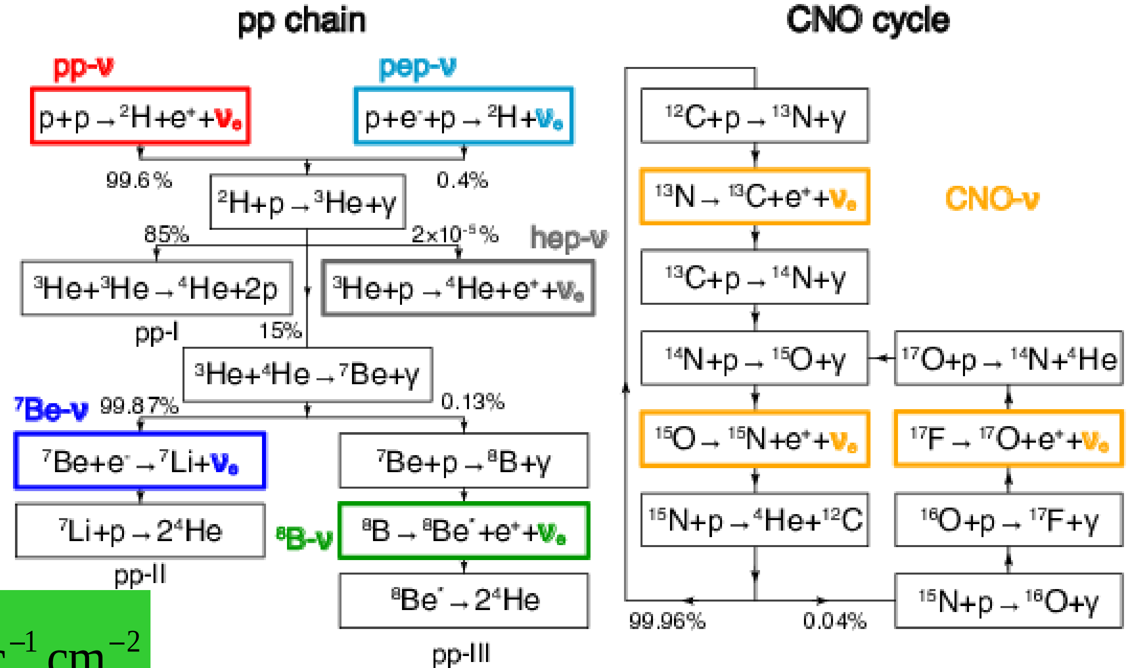

$$\Phi_\nu = \frac{2L_{sun}}{25\text{MeV}} \frac{1}{4\pi(1\text{AU})^2} = 7 \cdot 10^{10}\ \text{sec}^{-1}\ \text{cm}^{-2}$$

Line sources : $cm^{-2}s^{-1}$

Continuum sources : $cm^{-2}s^{-1}MeV^{-1}$

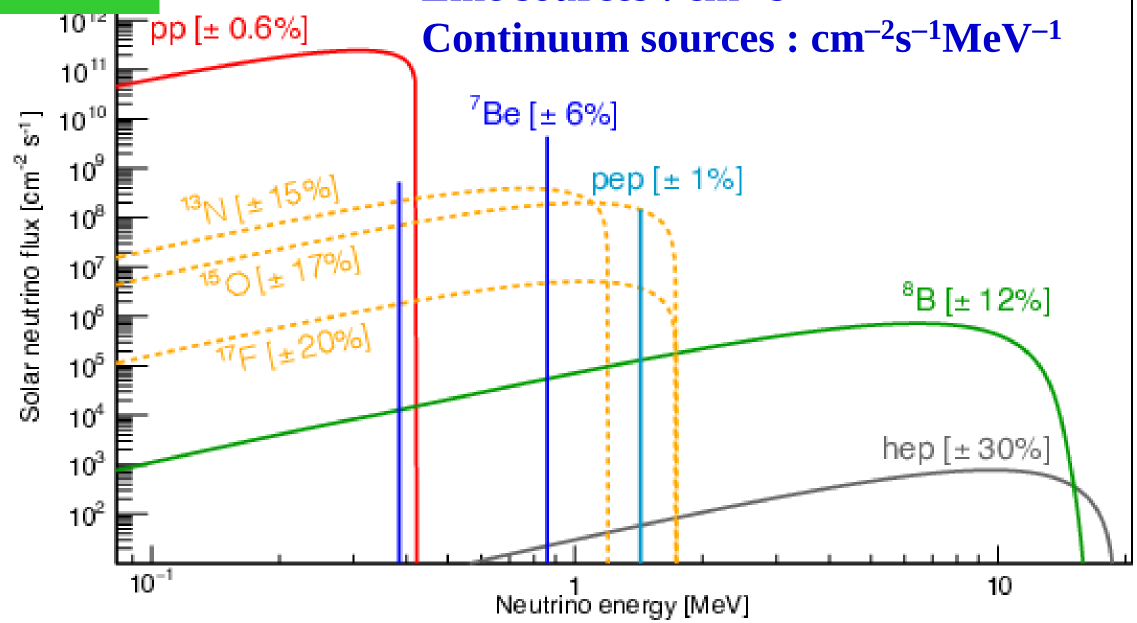

Primary aim : Precise measurement of the individual neutrino flux

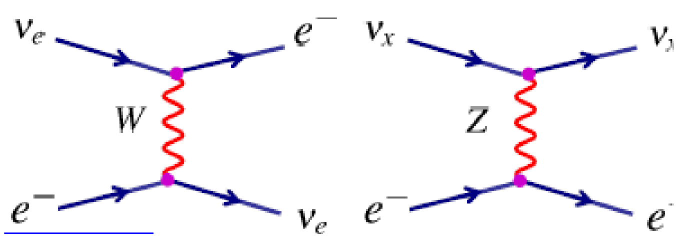

But, only few tens of counts per days in 100t of scintillator

Geo-neutrinos

Electron-antineutrinos from natural radioactive decays

$\bar{\nu}_e$: $4.1 \times 10^6/\mathrm{cm}^2/\mathrm{sec}$

Anti-neutrino Detector (e.g. Borexino)

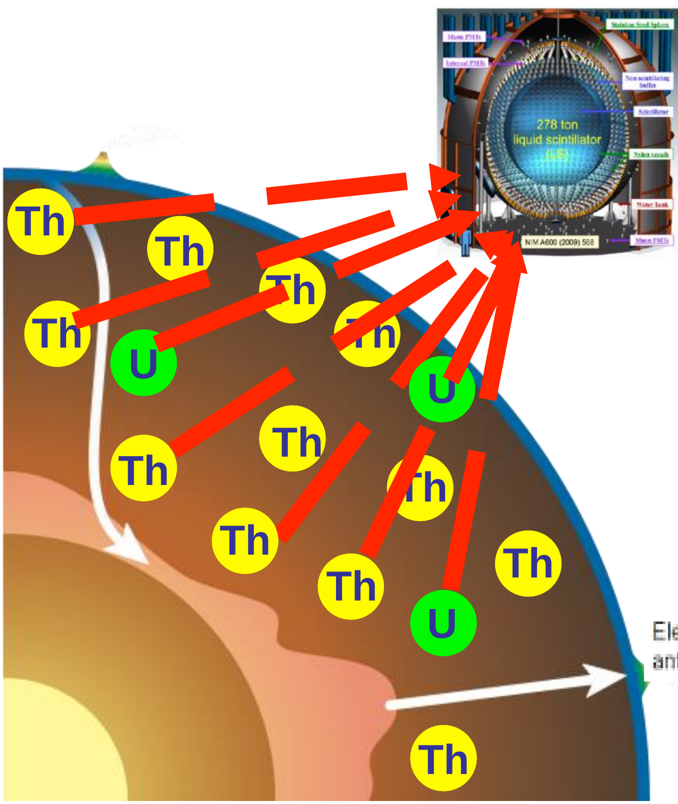

	$T_{1/2}$ (year)
$^{238}U \rightarrow {}^{206}Pb + 8\alpha + 8e^- + 6\,\bar{\nu}_e + 51.7\ MeV$	4.468×10^9
$^{235}U \rightarrow {}^{207}Pb + 7\alpha + 4e^- + 4\,\bar{\nu}_e + 46.4\ MeV$	7.040×10^8
$^{232}Th \rightarrow {}^{208}Pb + 6\alpha + 4e^- + 4\,\bar{\nu}_e + 42.7\ MeV$	1.40×10^{10}
$^{40}K \rightarrow {}^{40}Ca + e^- + \bar{\nu}_e + 1.31\ MeV$ (89.3%)	1.248×10^9
$^{40}K + e^- \rightarrow {}^{40}Ar + \nu_e + 1.505\ MeV$ (10.7%)	1.248×10^9

inverse β-decay

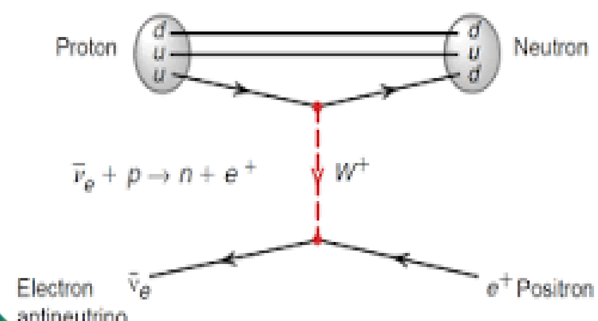

Energy threshold, 1.8 MeV

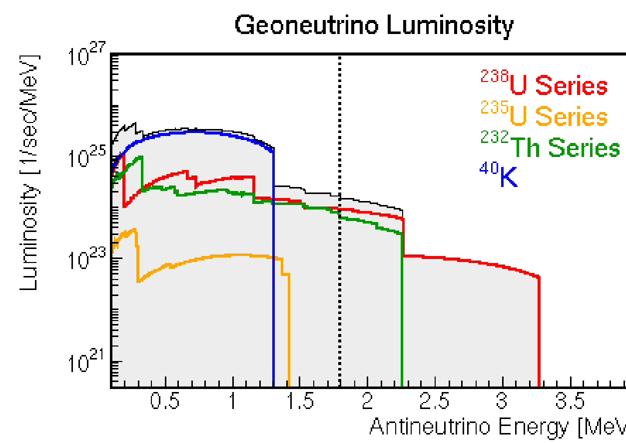

* Only geo-neutrinos from U and Th are detectable right now

* ^{40}K geo-neutrino detection needs new technology.

Number of geo -$\bar{\nu}_e$: Amount of U and Th, Radiogenic heat

Borexino: the quest for the radiopurity Grail

Requirements: since the neutrino signal is virtually indistinguishable from background, radiopurity is a MUST

- **The expected rate of solar ν in BX (in the energy window considered) is at most ~ 100 counts/day/100t which corresponds to ~ 5 10^{-9} Bq/Kg;**
- **Just for comparison of natural sources (~10^4 to 10^5 decays/ton/sec):**
  - **Natural water is ~ 10 Bq/Kg in ^{238}U, ^{232}Th and ^{40}K**
  - **Air is ~ 10 Bq/m^3 in ^{39}Ar, ^{85}Kr and ^{222}Rn**
  - **Typical rock is ~ 100-1000 Bq/m^3 in ^{238}U, ^{232}Th and ^{40}K**

BX scintillator must be 9 order of magnitude less radioactive than anything on Earth!

Source	Standard material	Phase-I scintillator (IV)	Phase-II (CNO) scintillator
^{238}U	$(6.6 \pm 1.9) \times 10^{-8}$ g/g	$(3.5 \pm 0.05) \times 10^{-18}$ g/g	$< 9.4 \times 10^{-20}$ g/g (90%CL)
^{232}Th	$(3.2 \pm 0.3) \times 10^{-8}$ g/g	$(3.8 \pm 0.8) \times 10^{-18}$ g/g	$< 5.7 \times 10^{-19}$ g/g (90%CL)
^{40}K	$(1.6 \pm 0.4) \times 10^{-5}$ g/g	$\sim 10^{-14}$ g/g	

Signal and background in Borexino expt

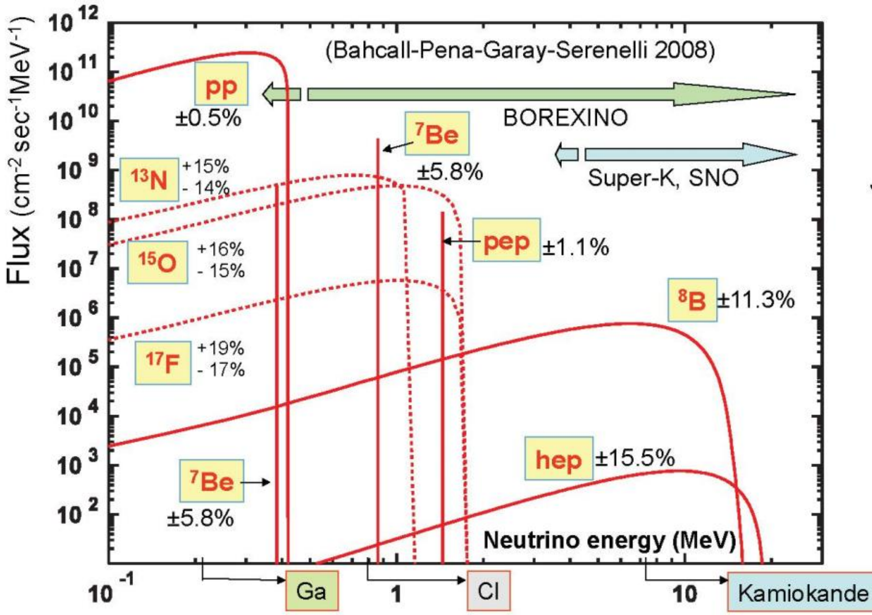

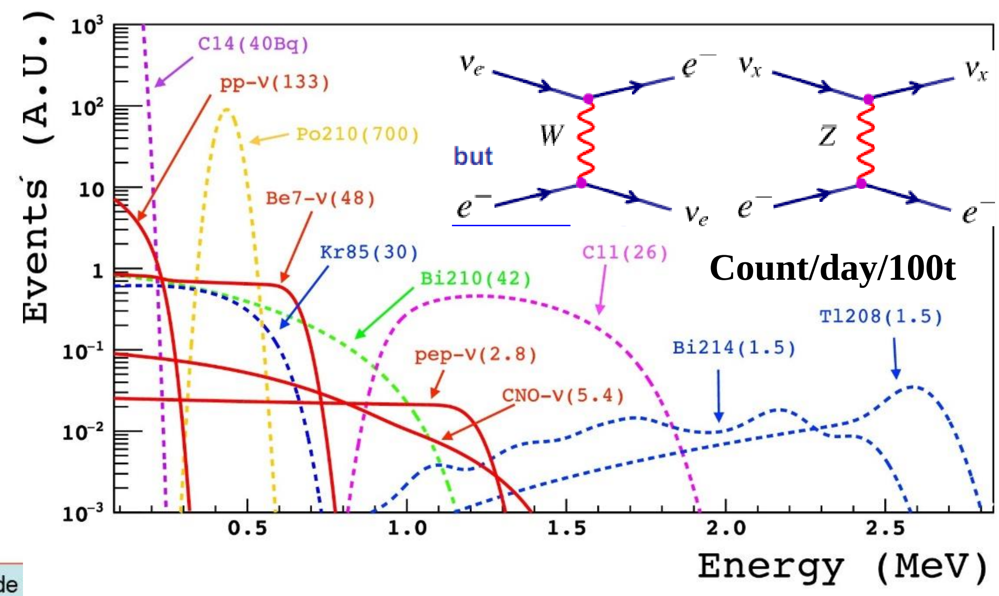

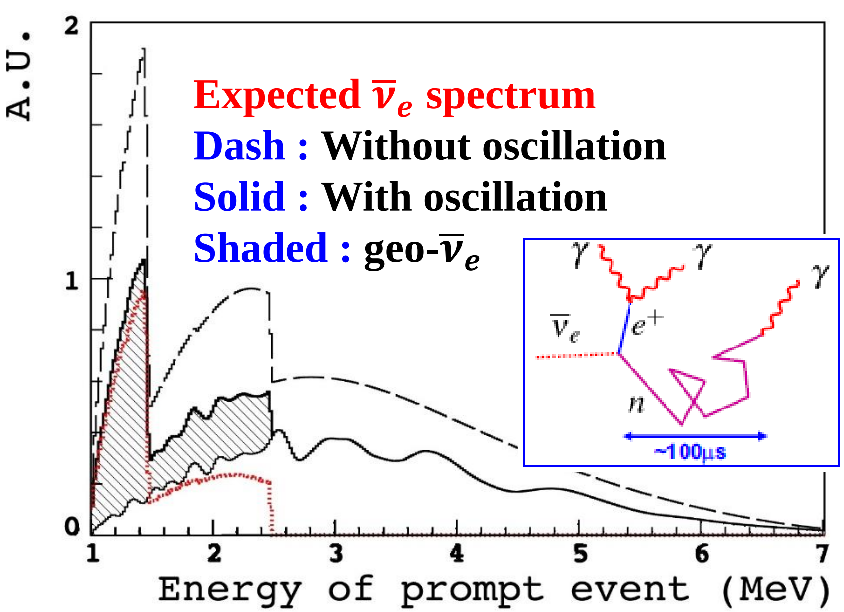

- **Meticulous energy calibration**
- **Under- standing of the degree of uniformity of the energy response of the detector over its volume,**
- **Trigger efficiency,**
- **Detector stability over time,**
- **Spatial reconstruction and time response for events of different type occurring at different positions, including the scintillation pulse shape characteristics.**

Signal and background events

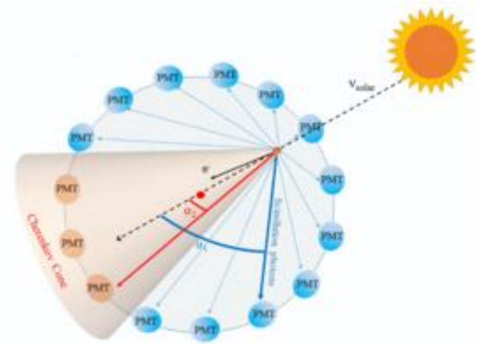

Solar neutrino events

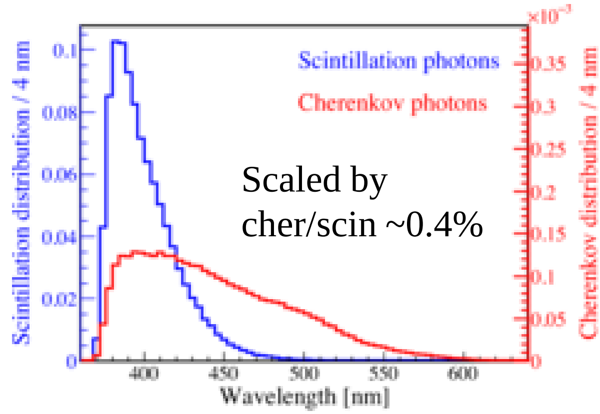

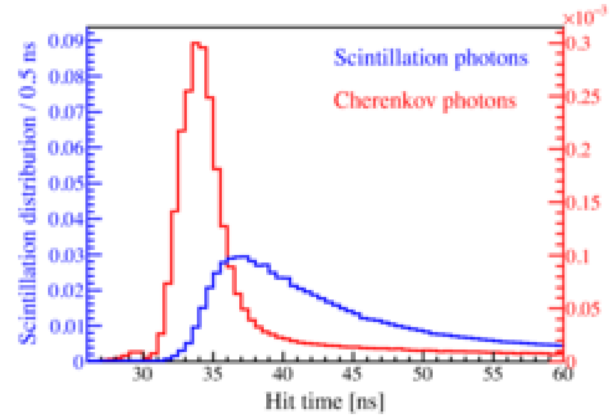

Radioactive bkg

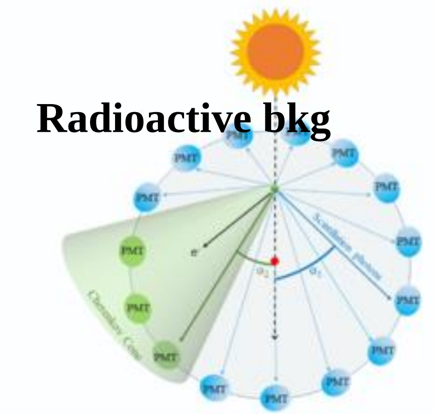

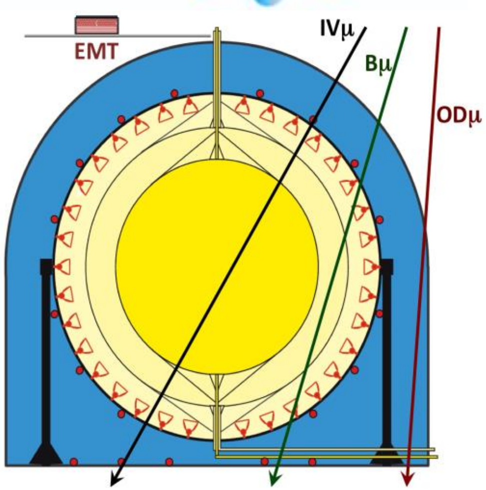

the Cherenkov cone of a muon that is crossing the curved surface of the SSS

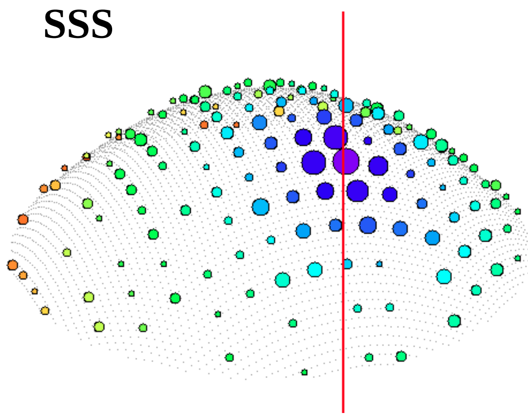

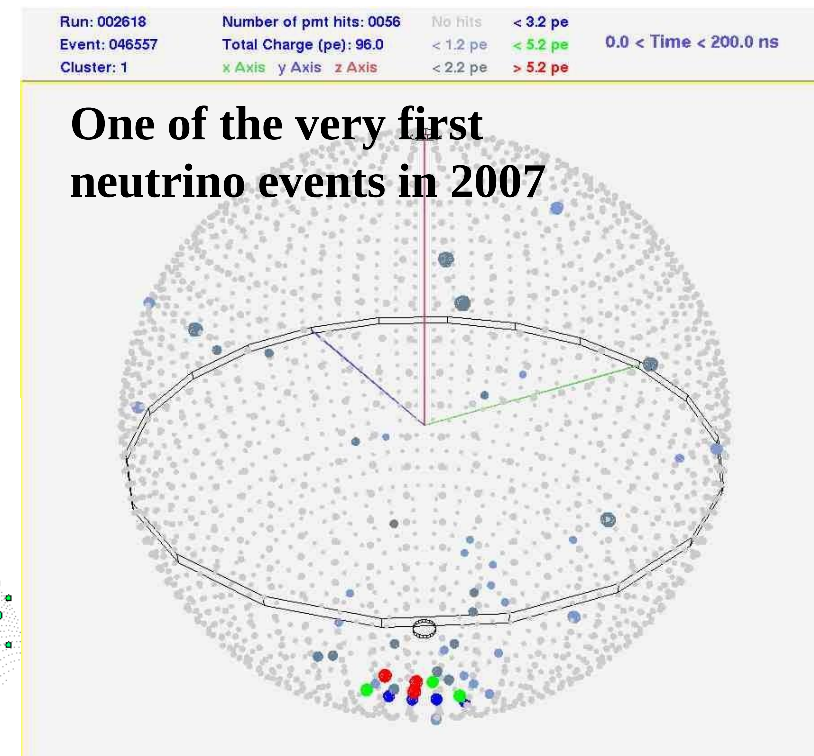

One of the very first neutrino events in 2007

BOREXINO Source Calibration

- 12 different sources were deployed in 295 locations
- The measurement of the position reconstruction accuracy and resolution for events distributed in the whole inner vessel and over the energy range.
- The calibration of the absolute energy scale and resolution especially in the energy region of interest for studying ^{7}Be , pep , and pp solar neutrinos interactions (i. e. ~100 keV - ~1.5 MeV).
- The measurement of the non-uniformity of the energy response as a function of the event position and energy.
- The production of signals mimicking the external background.

The neutron scattering during the thermalization and its subsequent capture by protons or nuclei are directly managed by the Geant4 libraries as well as the de-excitation of the daughter nucleus.

Isotope	Type	Energy (KeV)
^{57}Co	γ	122
^{139}Ce	γ	165
^{203}Hg	γ	279
^{85}Sr	γ	514
^{54}Mn	γ	834
^{65}Zn	γ	1115
^{60}Co	γ	1173,1332
^{40}K	γ	1460
^{222}Rn	α/β	0 - 3200
^{14}C	β	~0 - 156
^{241}Am-^{9}Be	n	~0 – 10,000
	γ (H)	2333
	γ (^{12}C)	4946
Ext. ^{238}Th	γ	2615

BOREXINO Source Calibration

- 12 different sources were deployed in 295 locations
- The measurement of the position reconstruction accuracy and resolution for events distributed in the whole inner vessel and over the energy range.
- The calibration of the absolute energy scale and resolution especially in the energy region of interest for studying ^{7}Be , pep , and pp solar neutrinos interactions (i. e. ~100 keV - ~1.5 MeV).
- The measurement of the non-uniformity of the energy response as a function of the event position and energy.
- The production of signals mimicking the external background.

The neutron scattering during the thermalization and its subsequent capture by protons or nuclei are directly managed by the Geant4 libraries as well as the de-excitation of the daughter nucleus.

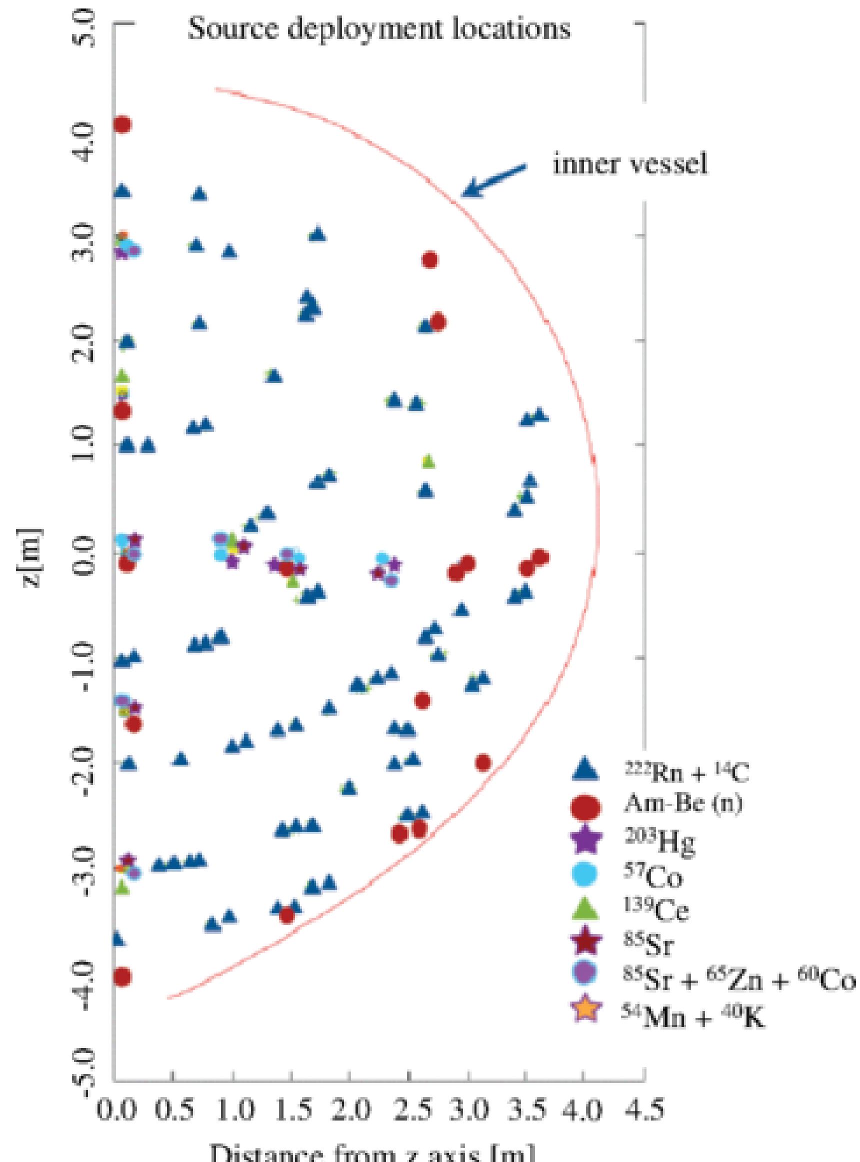

Ext. ^{238}Th	γ	2615

Borexino Simulation Chain

- Provide a wide range of event generators, from solar neutrino interactions, to radioactive decays, geo-neutrinos, and calibration source events.
- Simulate the energy loss of each specific particle in every material present in the detector, either active (the scintillator, buffer liquid, and water in the muon detector) or passive.
- Generate a number of scintillation ($\sim 10^4$ γ/MeV) or Čerenkov photons considering the particle energy loss in the media and the properties of the scintillator and/or the buffer.
- Track each single optical photon including its interactions with the scintillator and with the materials (absorption, reemission, scattering, reflection), until a PMT is reached or the photon is absorbed.
- Generate the PMT response for photons absorbed at the PMT cathode, considering the quantum efficiency of each individual PMT.
- Generate the PMT pulse signal taking into account the specific design of the front end and of the digital electronics chain of Borexino.
- Simulate the trigger generation and save the final output for triggering events.
- Produce a raw data file with the same structure as the one produced by the Borexino data acquisition system.

Leak and concentration of quencher

- The OV and IV themselves block the inward transfer of Radon emanated from the internal PMTs and SSS.
- The quencher concentration has been varied twice, changing it from the initial 5 g/l to 3 g/l and then to 2 g/l , with negligible consequences on the buffer's optical behavior.
- These operations have reduced the density difference between the buffer and the scintillator in order to minimize the scintillator leak (appeared in April 2008, with a location estimated as $26° < \theta < 37°$ and $225° < \phi < 270°$) from the central volume through the small hole in the IV to the IB as much as possible.

- This campaign was mostly successful, but the IV shape has become non-spherical and changing in time.
- Dynamical fiducial volume (DFV) is defined along the time-dependent (average of 7-days) reconstructed IV shape.
- The precision of determination of IV boundary is found to be ~1% (±5 cm).

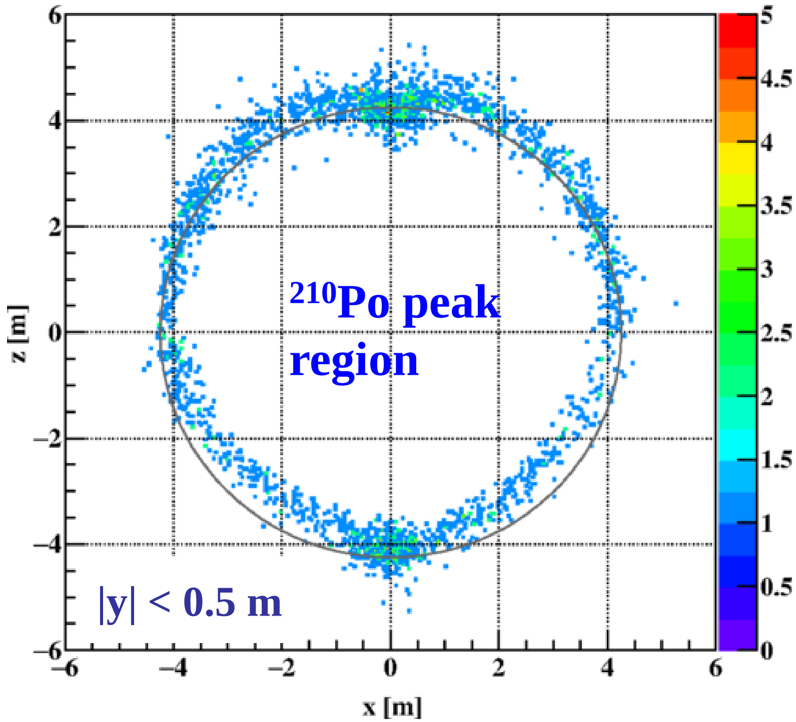

Outer Detector Geometry in Geant4

Simulated Geometry

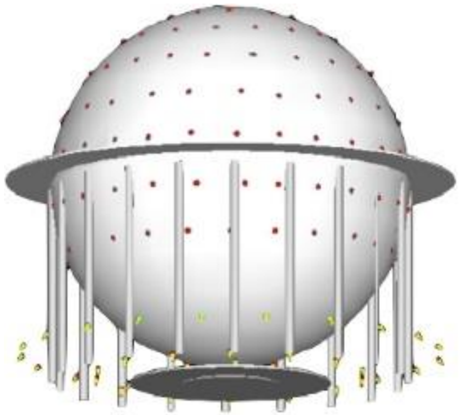

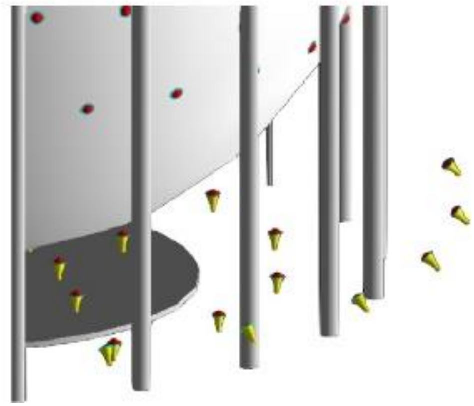

PMT

Simulation

real object

- **Reflective tyvek foils cover the surface leaving free only the photocathodes facing the water.**
- **The tyvek foils placed on the inner surface of the water tank.**
- **Main points in simulation**
  - **Tyvek reflectivity dependence upon the wavelength,**
  - **PMT quantum efficiencies,**
  - **Water properties.**

Inner Detector Geometry in Geant4

Simulated Geometry

The realistic inner vessel is updated on weekly basis

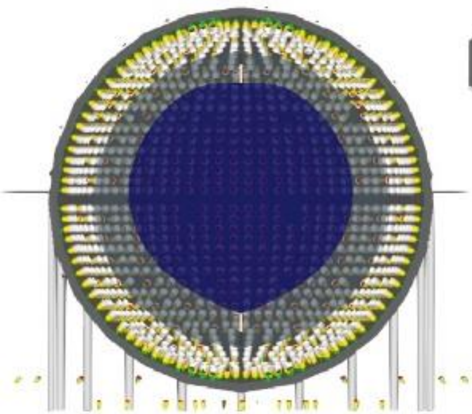

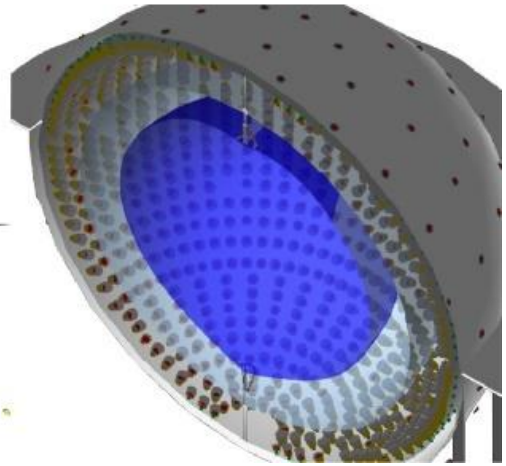

Inner detector PMT

Real object **Simulation**

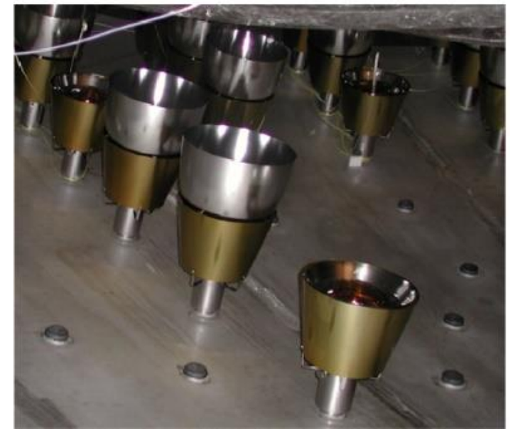

- **The real vessel shape is simulated can be adjusted by the user with optimal values usually around ~5 cm (i. e. the shape is approximated with a polygonal shape in the r −θ plane with sides of ~5 cm).**

- **Wavelength dependent**
  - **Aluminium reflectivity of light concentrator**
  - **Nylon vessel absorption length and its refractive index**
  - **Specular and diffused reflection**

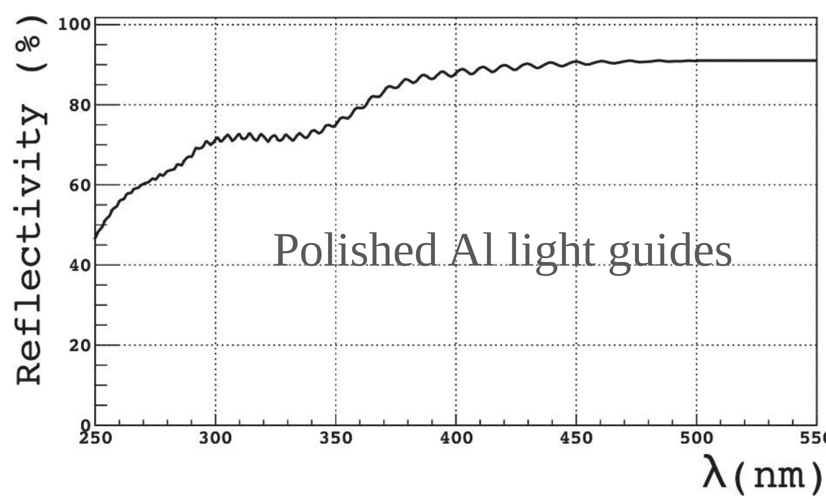

Generation of scintillation light

- $\frac{dY^{ph}}{dx} = \frac{Y_0^{ph}\, dE/dx}{1+k_B \cdot dE/dx}$, $Y_0^{ph} \approx 10^4\ \gamma/MeV$ and k_B ~0.01 cm/MeV
- Quenching factor $Q_p(E) = \frac{1}{E}\int_0^E \frac{dE}{1+k_B \cdot dE/dx}$
  p $=\{\alpha, \beta, \gamma\}$
- $Y_p^{ph}(E) = Y_0 \cdot Q_p\,(E) \cdot E$
- The quenching effect is relevant for γ also.
- $Y_\gamma(E) = Y_0 \sum_i E_i\ Q_\beta(E_i) = Y_0 \cdot Q_\gamma(E) \cdot E < Y_\beta(E)$
  – $Y_\gamma^{ph}(256\ KeV) = Y_\beta^{ph}(220\ KeV)$
- Light emission time, t, $P(t) = \sum_{i=1}^{4} \frac{w_i}{\tau_i} exp(-t/\tau_i)$
  – w_i & τ_i depends on type of particle (β, γ)
- Scintillation time constant in buffer is 2.8ns and spectrum is similar to PC, but only 4% of inner vol

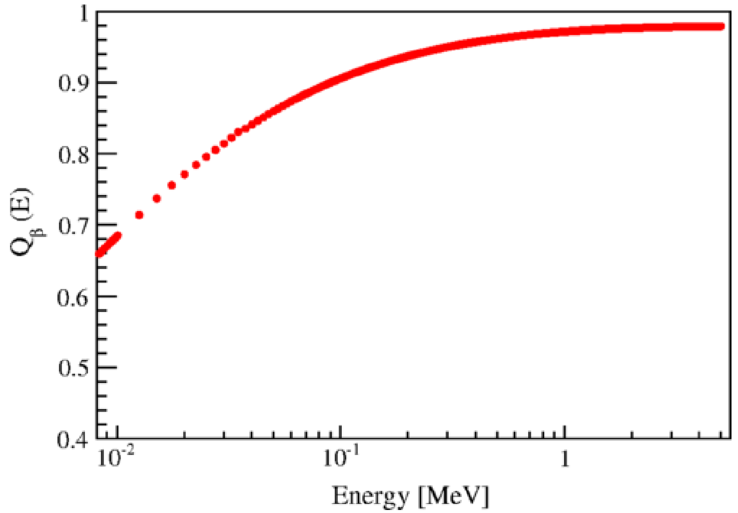

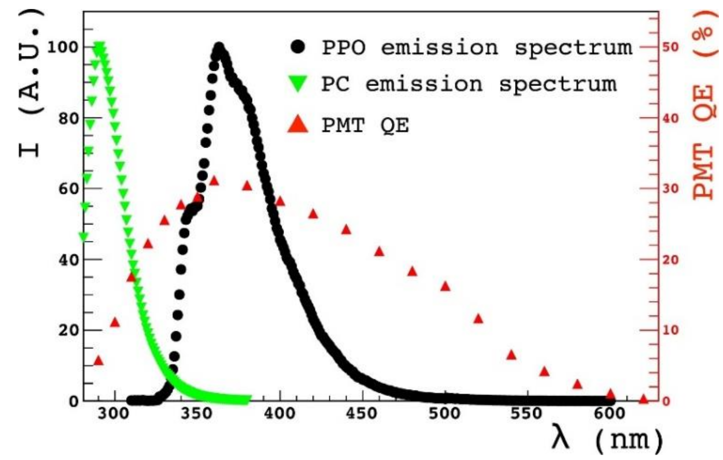

Generation of Cherenkov light

- $\frac{d^2N}{dx\,d\lambda} = \frac{2\pi\alpha}{\lambda^2}\left(1 - \frac{1}{\beta^2 \cdot n^2(\lambda)}\right)$
- Attenuation length of UV light in very small (sub mm), but a fraction of remitted light is detected

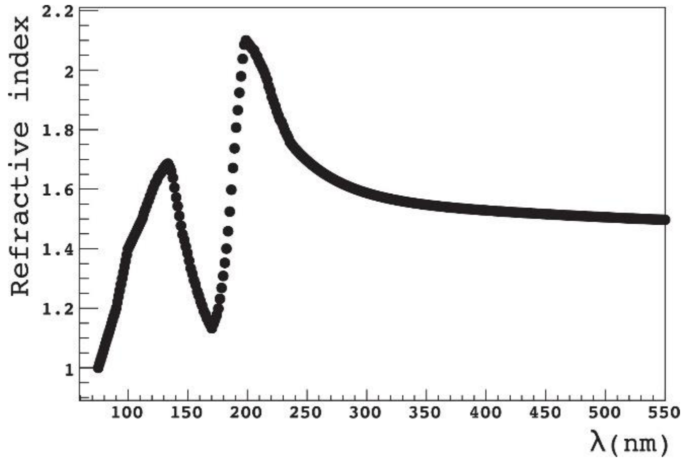

The light tracking

- **Elastic Rayleigh scattering ($P(\theta) = 1 + cos^2\theta$),**
- **Absorption and reemission of photons by PPO molecules,**
- **Absorption of photons by DMP,**
- **Photon absorption in the thin nylon vessels.**

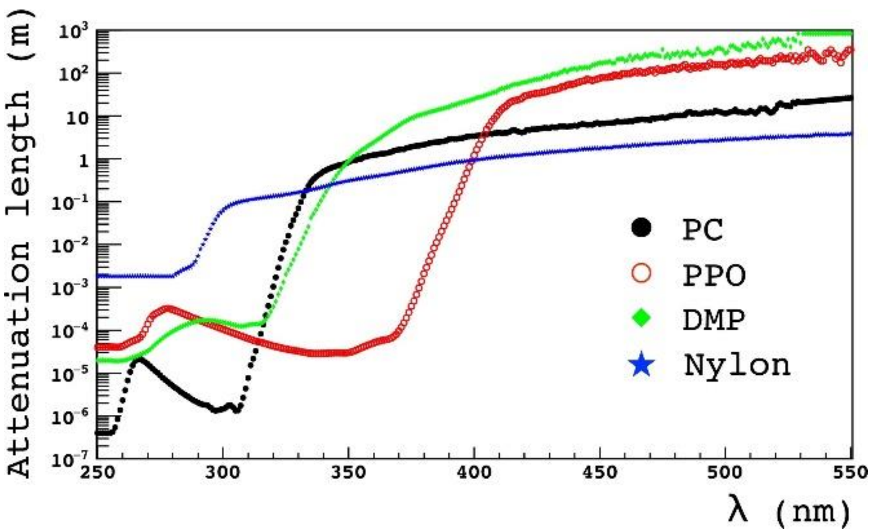

Remission prob in PPO	
λ (n)	**Reemission Prob**
λ < 320 nm	**0.53***
320 nm <λ<375nm	**0.839**
λ > 375nm	**0.15**

- $\tau_{PPO} = 1.6ns$
- $\tau_{PCtoPPO} = 3.6ns$
- $\tau_{PC} = 2.8ns$ **(in buffer)**

- **Elastic Rayleigh scattering, absorption and reemission of photons by PPO molecules, absorption of photons by DMP, and also photon absorption in the thin nylon vessels.**

Effective Quantum Efficiency

- The same spectral dependence of the quantum efficiency (QE), but different peak values, are assumed for all PMTs.

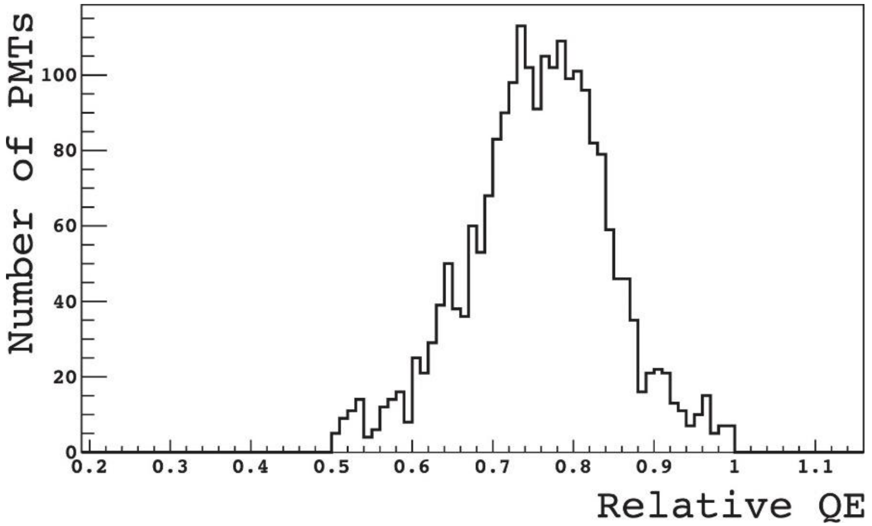

Simulation of readout e

- The typical dark noise rate is around a f of Hz for most of the PMTs.
- Time alignment is achieved by a commo precision of better than 0.5 ns.
- Input from data as weekly basis
  - Dark rate of individual PMTs
  - Effective quantum efficiency for each
  - PMT gains
  - Bad channels and detector inefficienci
- Digital board has a dead time of 140ns

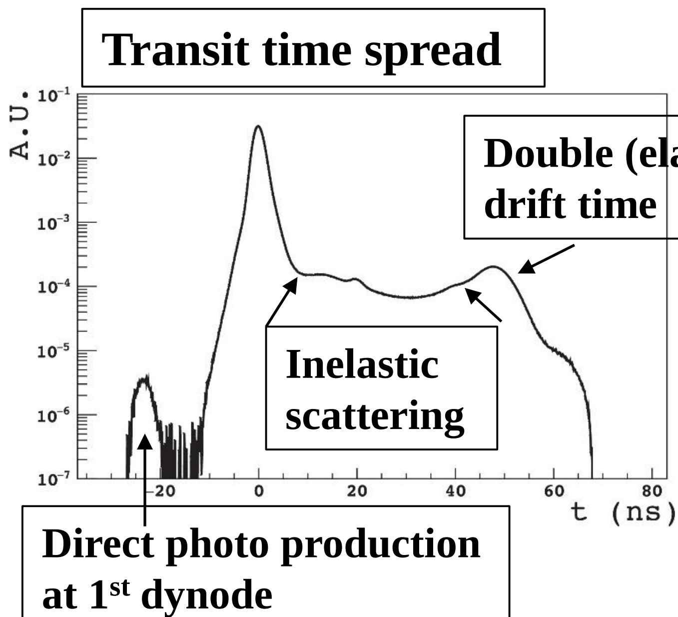

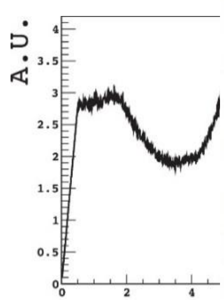

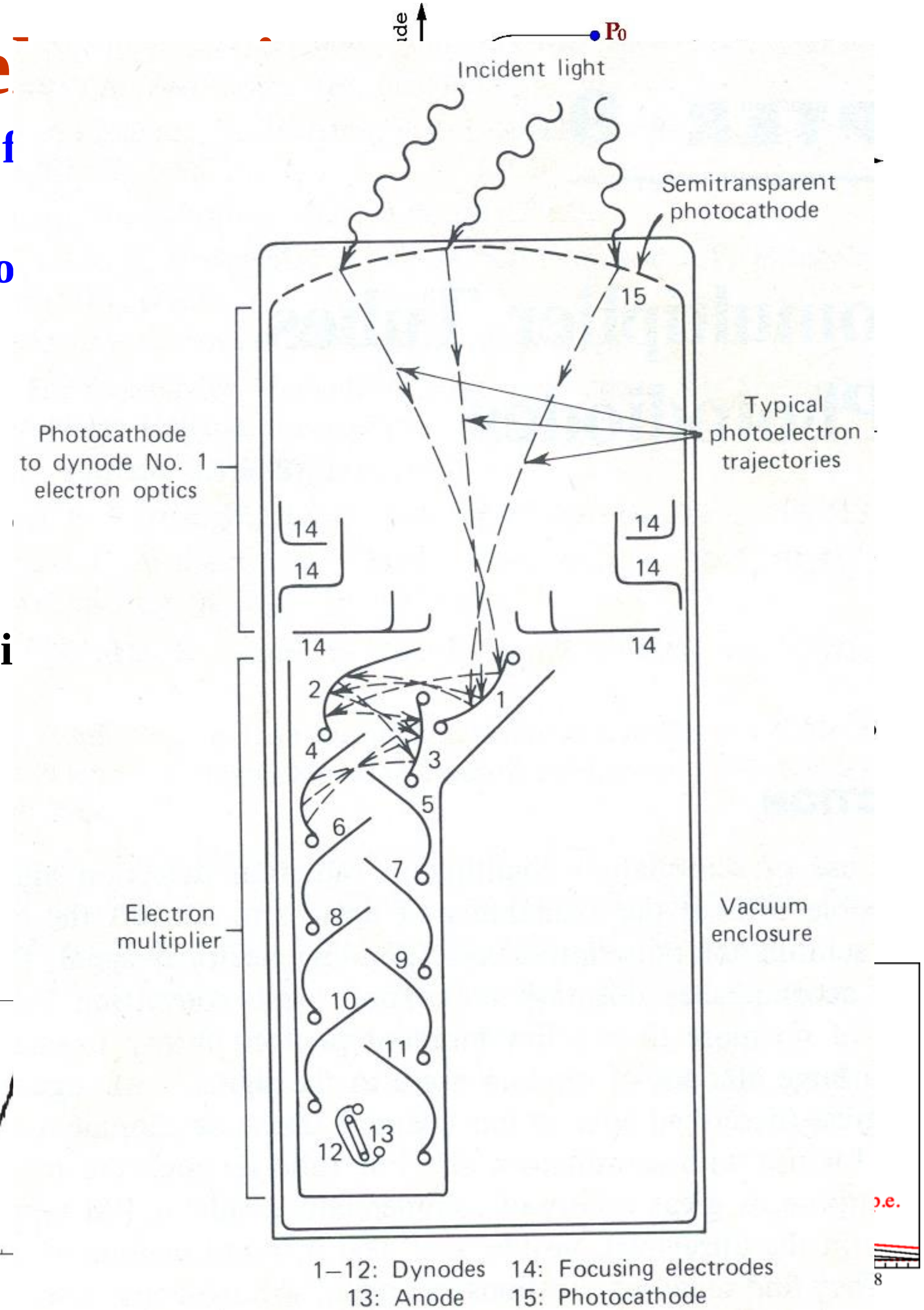

Simulation of readout electronics

- The typical dark noise rate is around a few hundreds of Hz for most of the PMTs.
- Time alignment is achieved by a common laser pulse, precision of better than 0.5 ns.
- Input from data as weekly basis
  - Dark rate of individual PMTs
  - Effective quantum efficiency for each channel,
  - PMT gains
  - Bad channels and detector inefficiencies
- Digital board has a dead time of 140ns

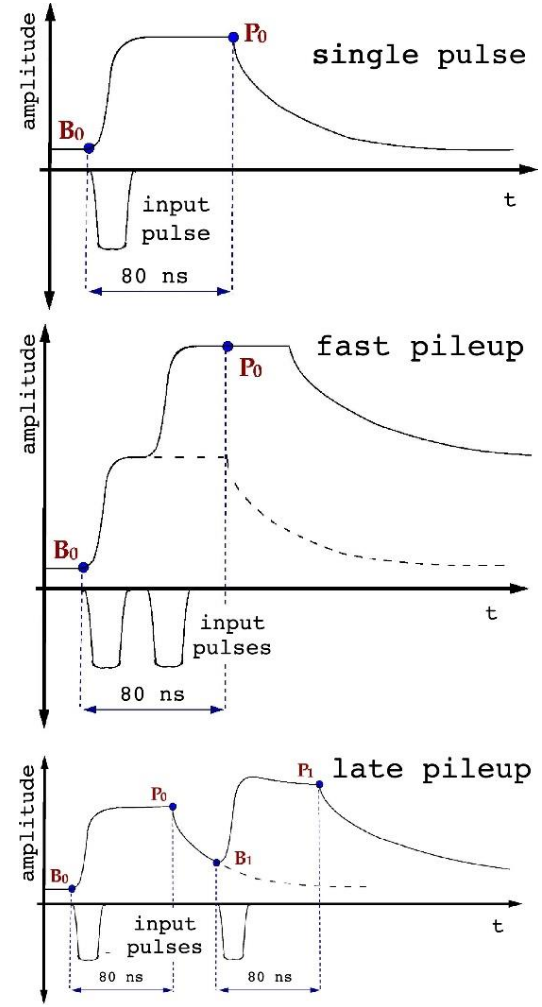

Transit time spread

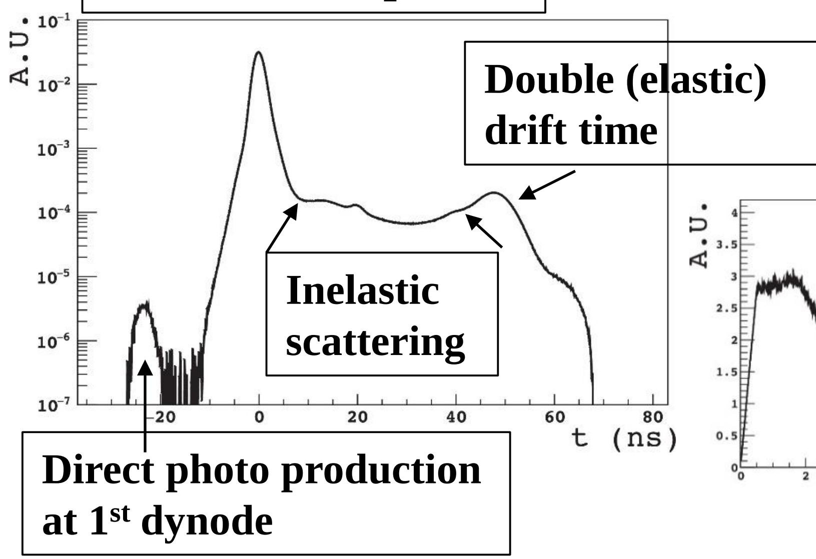

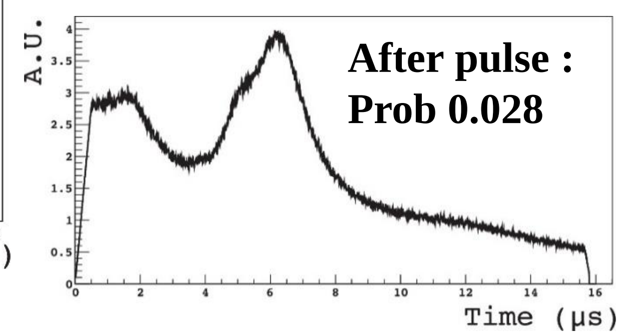

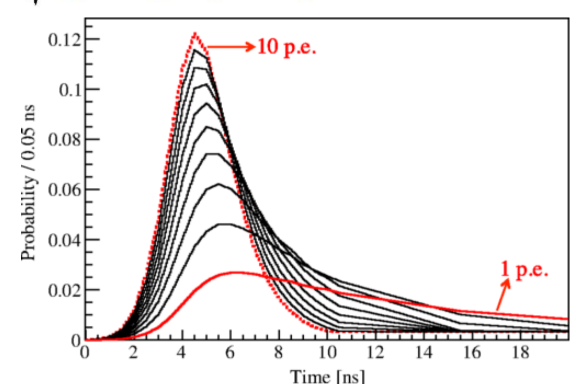

Reconstruction

- Typically, trigger threshold and time window are set to N = 20 - 30 and t = 100 ns .
- Trigger : all the hits within the acquisition gate of ~16.5 μs (~6.9 μs before Dec. 2007) are saved.
- Reconstructed objects
  - Number of hit PMTs, $N_p^m = \sum_{j=1}^{N'} p^j$
  - Number of hits, $N_h^m = \sum_{j=1}^{N'} h^j$
  - Normalised wrt to operating channel, N', $N_{p,h} = \frac{Ntot\ (=2000)}{N'(t)} N_{p,h}^m$
  - Similarly, number of p.e., $N_{pe}^m = \sum_{i=1}^{N_h^m} q_i^j$, $N_{pe} = \frac{Ntot\ (=2000)}{N''(t)} N_{pe}^m$
- Position reconstruction using $T_{flight}^j(\vec{r}_0, \vec{r}^j) = |\vec{r}_0 - \vec{r}^j| \frac{n_{eff}}{c}$ and then $L_E(\vec{r}_0, t_0 | \overrightarrow{(r^j, t_i^j)})$

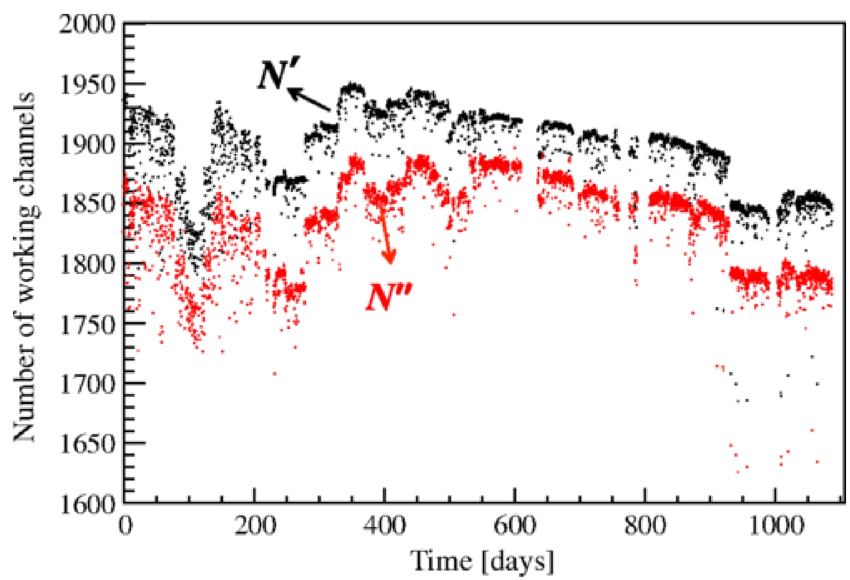

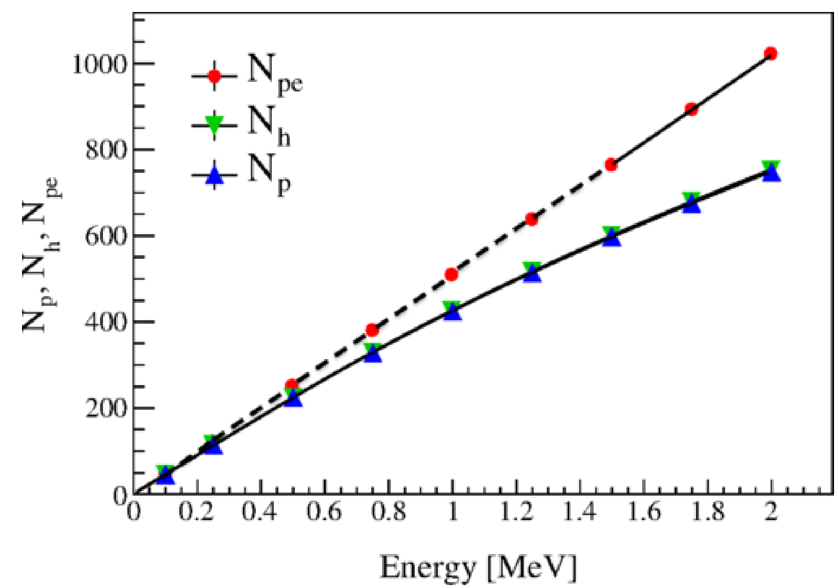

Tuning of MC

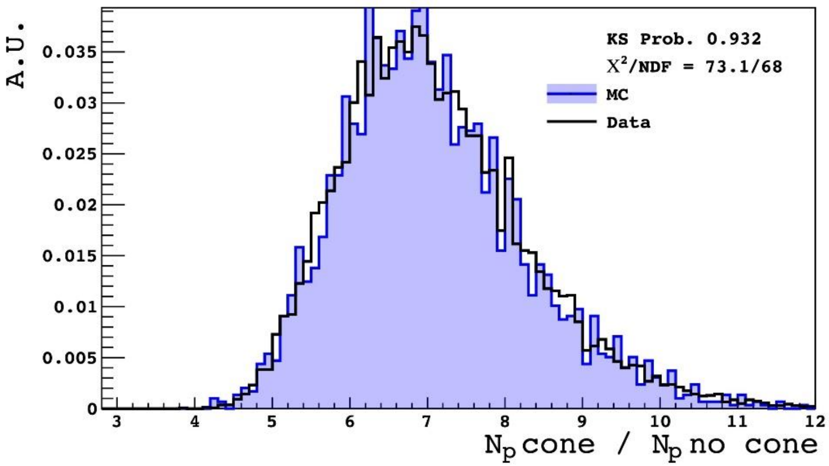
KS Prob. 0.932
X²/NDF = 73.1/68
MC
Data
A.U.
N_p cone / N_p no cone

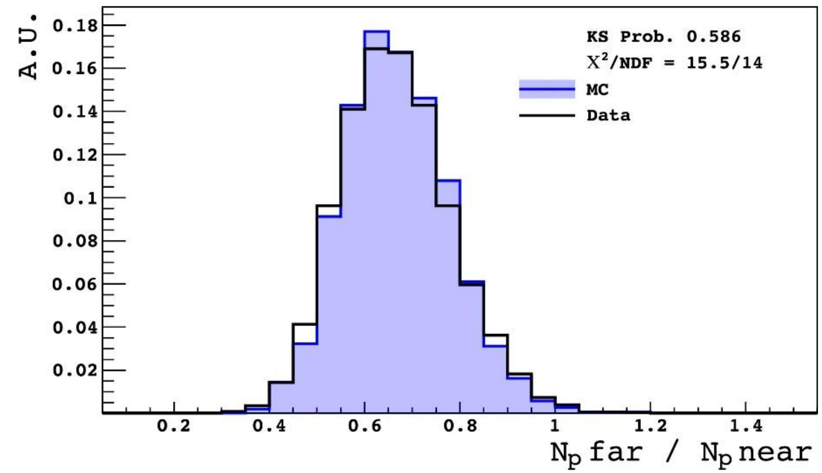
KS Prob. 0.586
X²/NDF = 15.5/14
MC
Data
A.U.
N_p far / N_p near

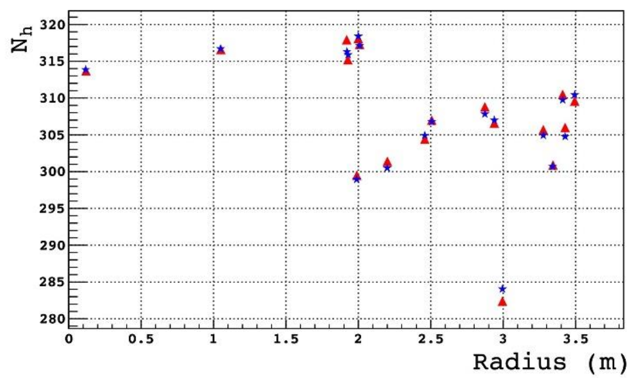
N_h
Radius (m)

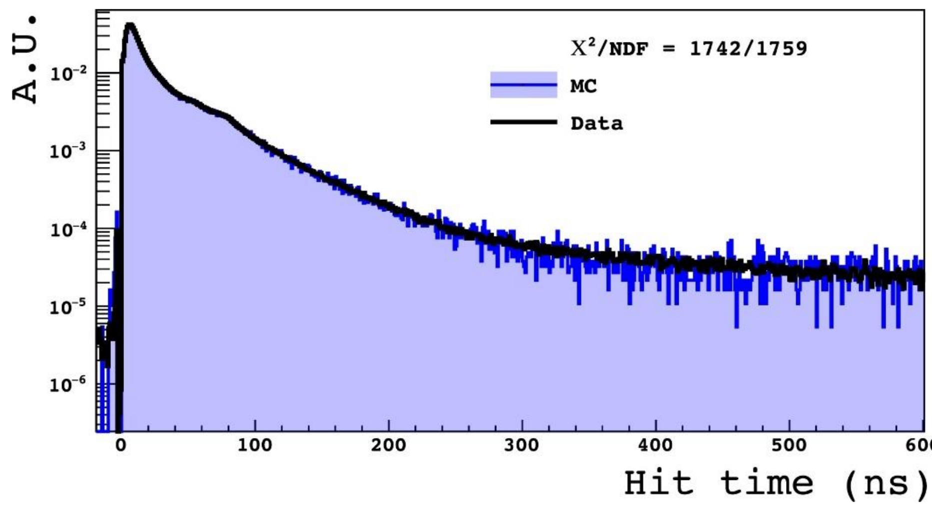
X²/NDF = 1742/1759
MC
Data
A.U.
Hit time (ns)

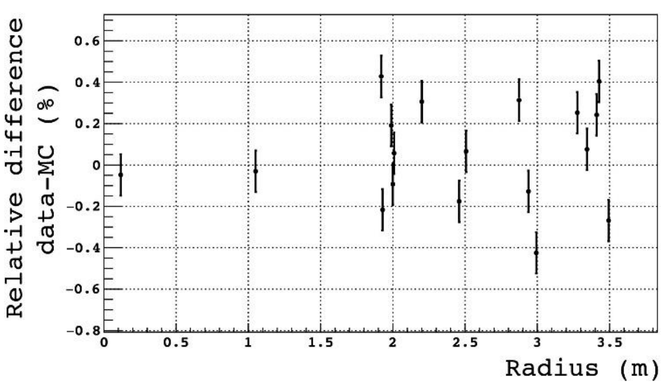
Relative difference
data-MC (%)
Radius (m)

Tuning of Energy scale and resolution

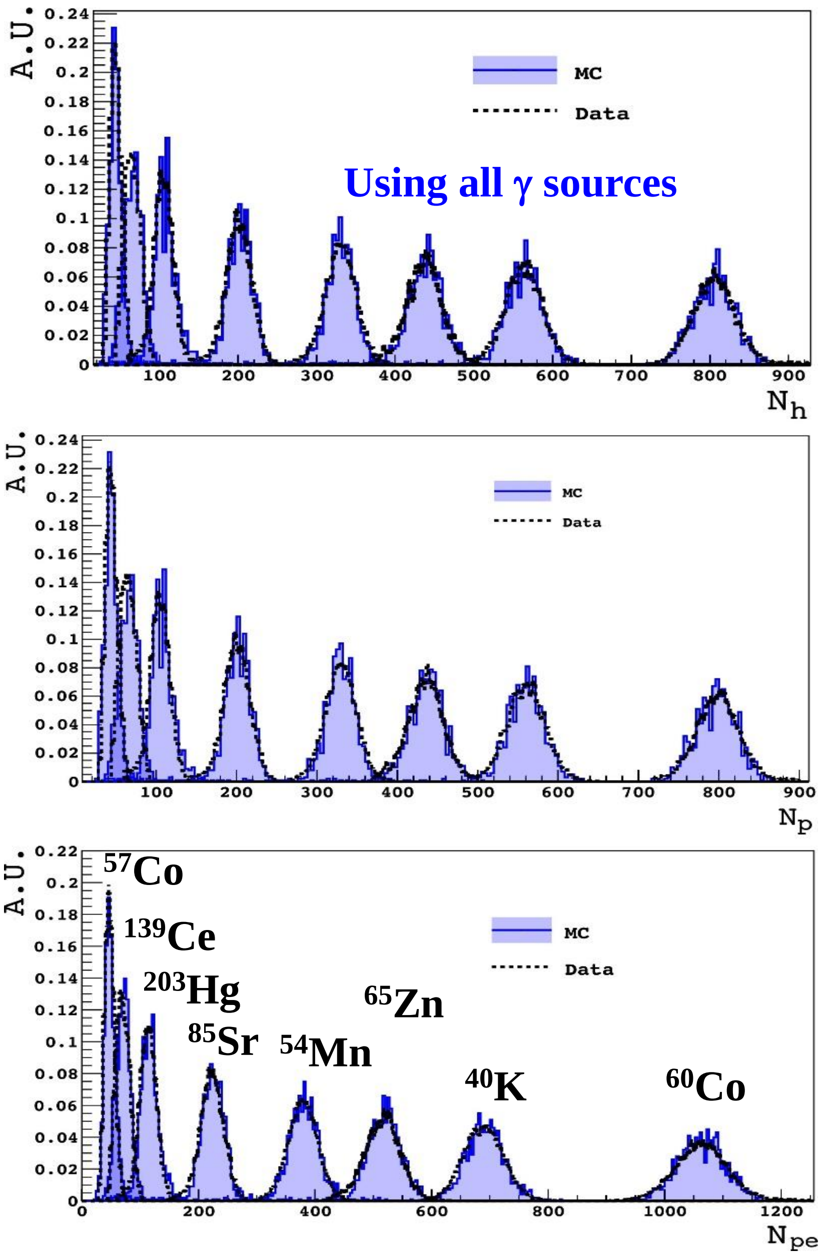

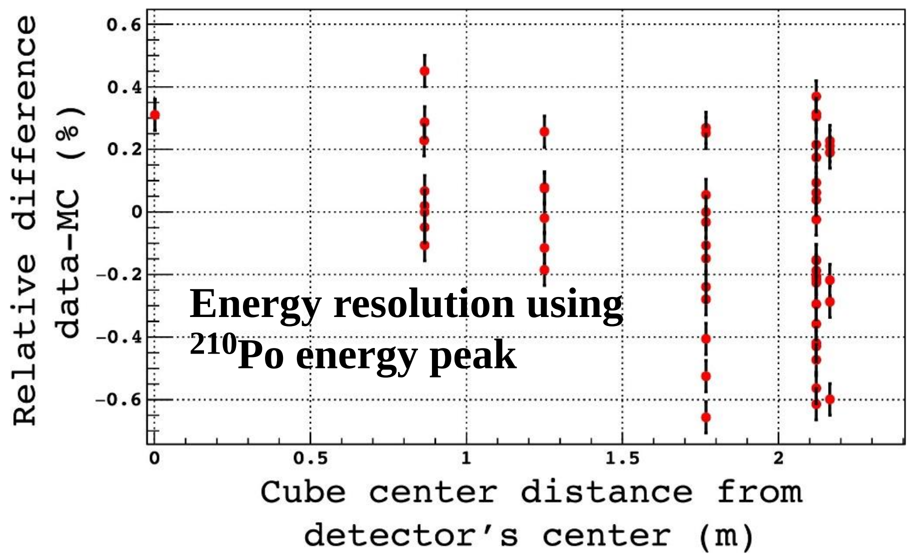

Results from tuning		
Parameter	Expected value	Tuned value
Y_0^{ph} (γ/MeV)	O(10^4)	13,600
k_B (β, cm MeV^{-1})	O(10^{-2})	0.01098
k_B (γ, cm MeV^{-1})	O(10^{-2})	0.01055
PMT Gain, G_S^{PMT}	1	1.015
P_{reem} (λ <320nm)	-	0.53

The Long History of Borexino

Purification I — **Purification II** — **Thermal insulation** — **Decommissioning**

2007 — **2010** — **2012** — **2016** — **2021**

Phase I (2007-2010) | Phase II (2012-2016) | Phase III (2016-2021)

- ν (^{7}Be) flux
- ν (^{8}B) flux
- ν (pep) flux
- ν (CNO) limit
- Limit on NMM

Improved radiopurity:
- ^{85}Kr: reduced by ~4.6
- ^{210}Bi: reduced by ~2.3
- Th and U negligible ($\sim 10^{-19}$ g/g)

- ν (pp) flux
- **New results on the solar fluxes***
- Neutrino magnetic moment limit
- Correlations with gravitational wave signals
- **Non-standard interactions (NSI)**

*Nature 562 (2018) 505

- **Geoneutrinos latest update**

- **CNO detection***

*Nature 587 (2020) 577

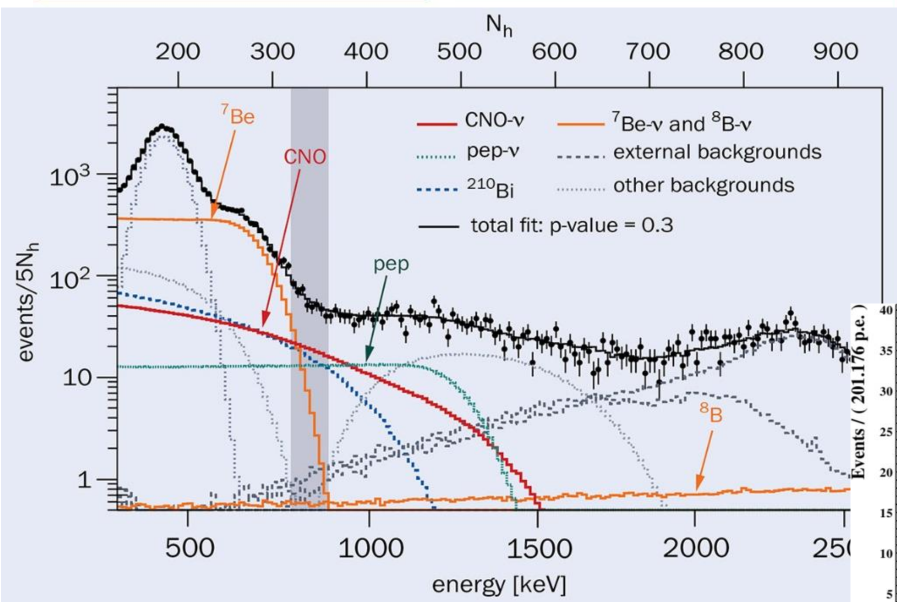

$\nu(\mathrm{CNO}) = 7.2\ ^{+2.9}_{-1.7}$ (stat) cpd/100t

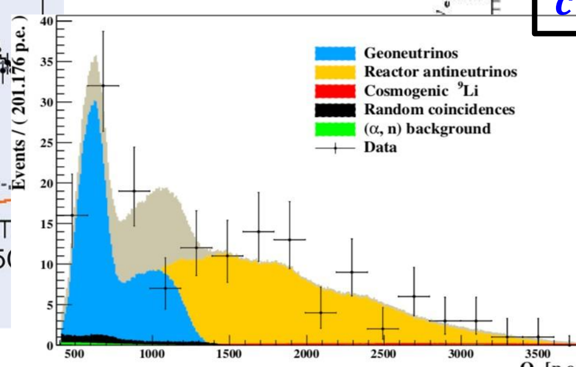

$P(\nu_e \rightarrow \nu_e) = (1/2)[1 + \cos(2\theta_N)\cos(2\theta_0)]$

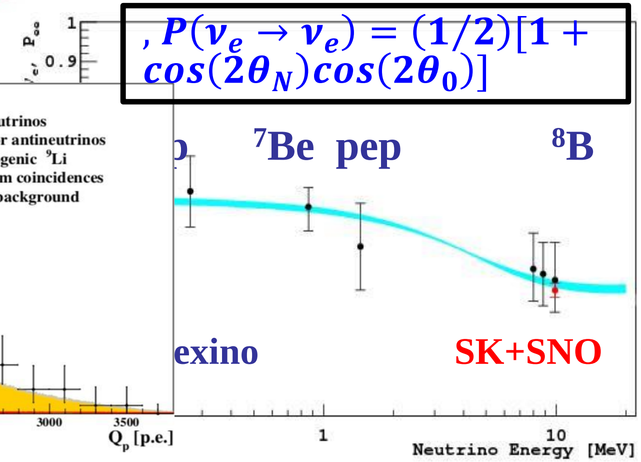

Simulation of atmospheric neutrino events

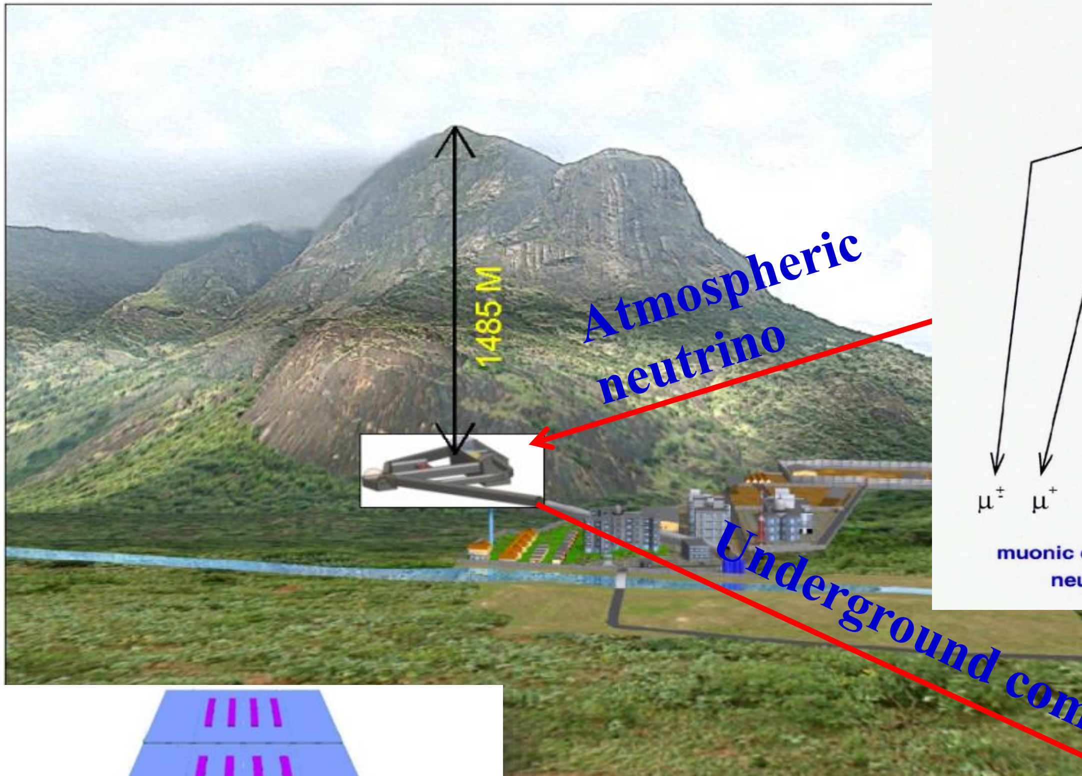

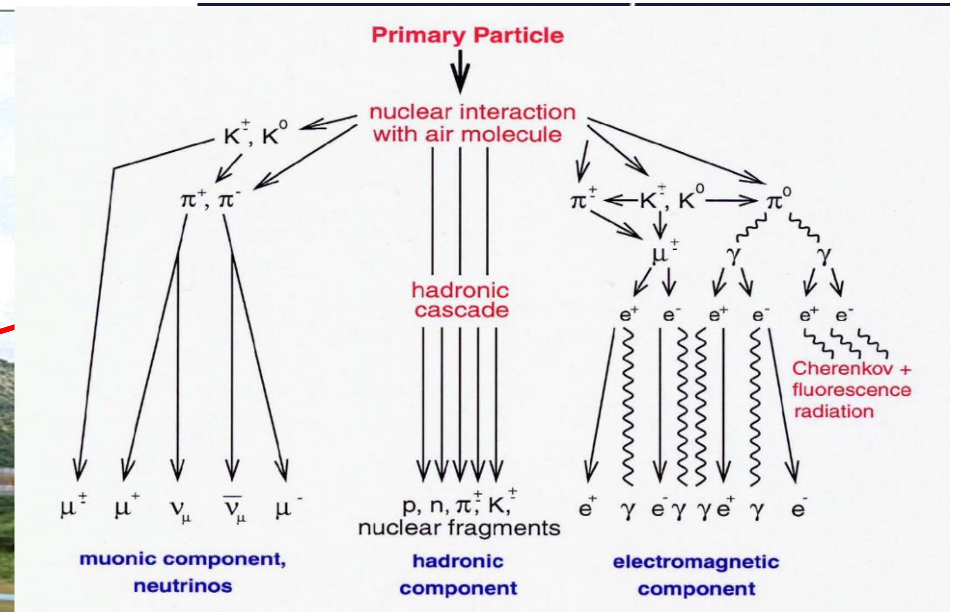

Underground complex

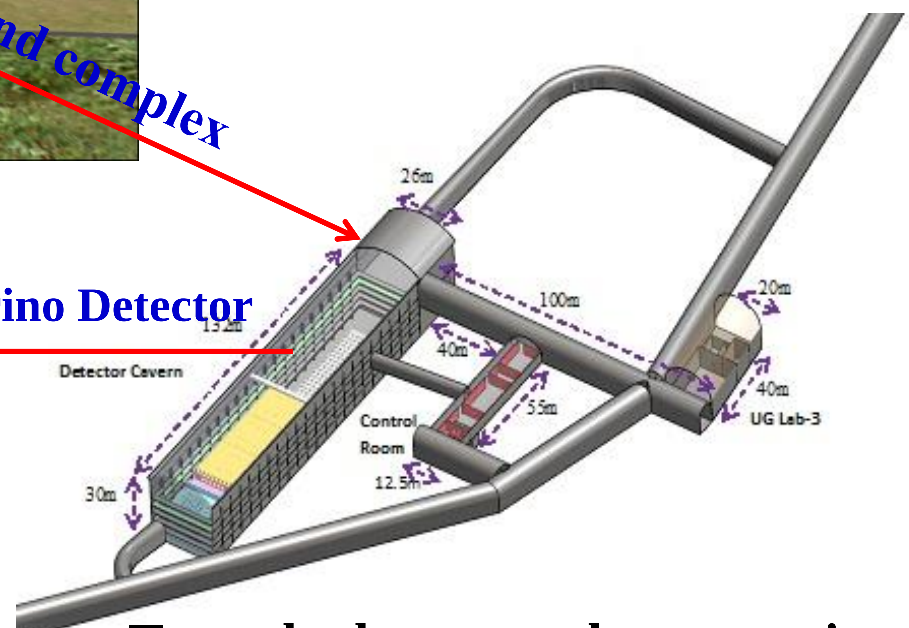

50Kton ICAL neutrino Detector

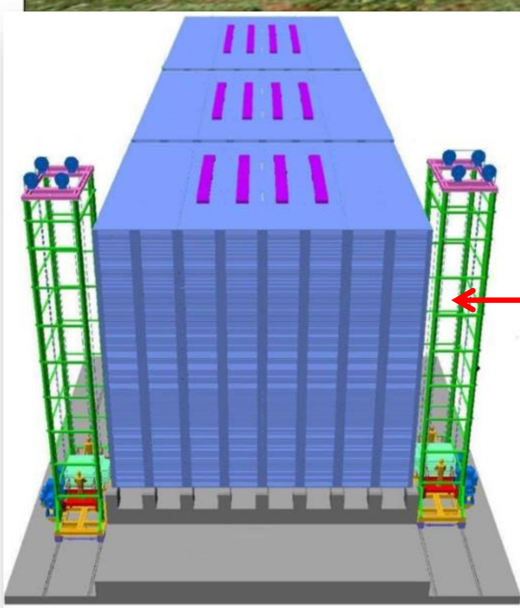

To study the atmosphere neutrino

Generation of cosmic neutrino interaction in detector material

- **External inputs :**

  1. Neutrino Flux table,

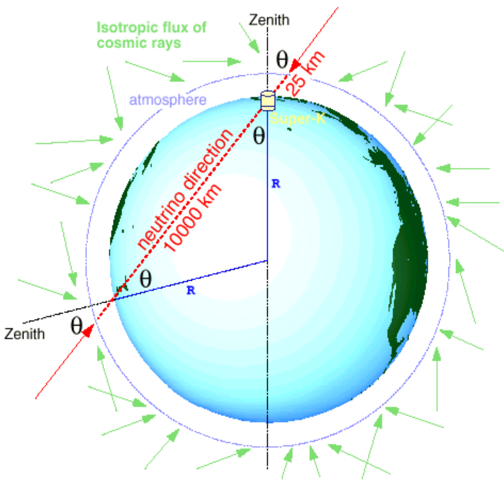

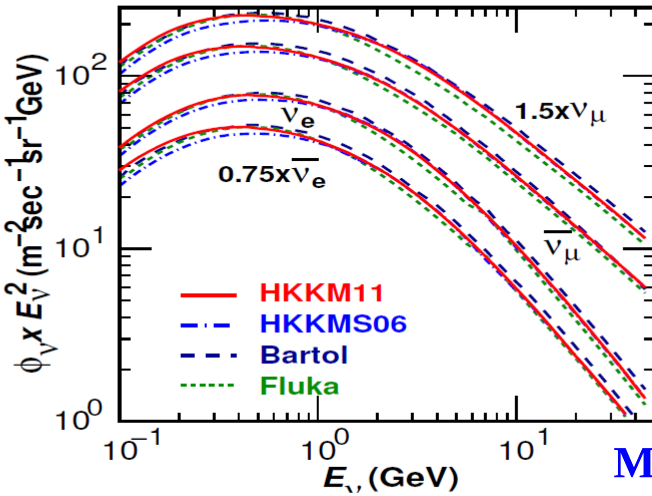

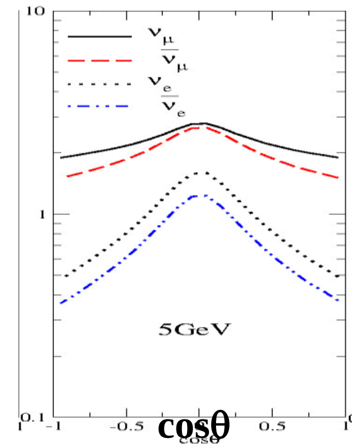

May include the oscillation to change flux of different flavour

$$P(\nu_e \rightarrow \nu_f; L, E) = \sin^2 2\theta \ \sin^2 \frac{1.27 \Delta m^2 L}{E}$$

2. Neutrino interaction cross-sections, neutrino-nucleon interaction,…

3. INO detector geometry (including electronics, support structures)

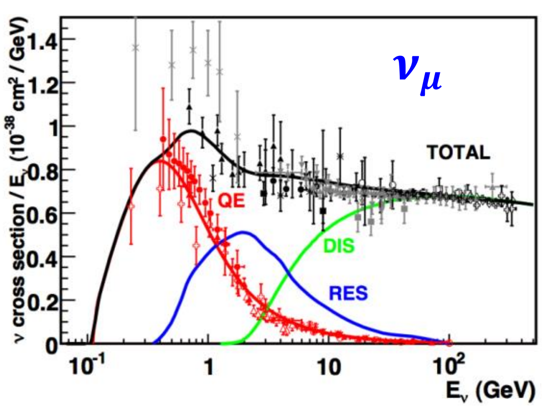

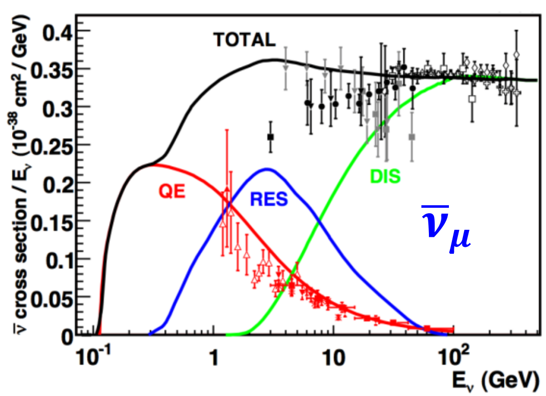

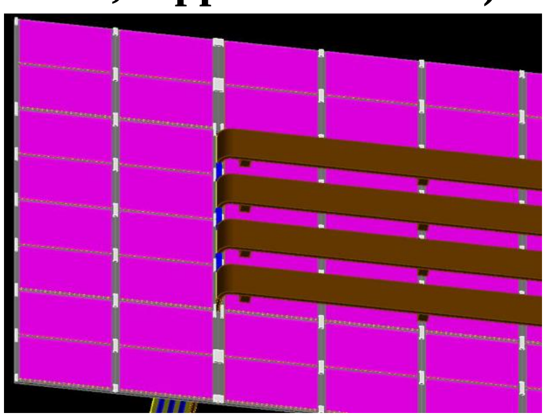

Neutrino event generation at INO

C Andreopoulos *et al*, *Nucl. Instrum. Methods* A 614 (2010) 87

- **Initialisation : Randomly look for many direction, e.g., 10^5 and estimate the maximum (P_{mx}) value of neutrino interaction probability, $\sum_{mat} \sigma(E) \times L \times N_A \times \rho$ for all neutrino flavours**
  - **(1) Calculate total event for a give exposure time**
- **Event Generation :**
  - **Select $E_\nu, cos\theta$ and ϕ ((2) 3D flux table) using combined flux table (simple acceptance and rejection method, (3) but change the weight to have high statistics at high E_ν)**
  - **Flux generation surface (πR_T^2) is outside the input geometry volume (distance R_L) for the given direction, to endure that detector is completely covered by the flux from the surface**
  - **Choose a random point on that surface**
  - **Compute Interaction Prob and whether accept or reject according to the ratio wrt to P_{mx}.**
  - **Material selection simply based on ($\sigma(E) \times L \times N_A \times \rho$) for different material**
  - **Selection of position is simply from the length**

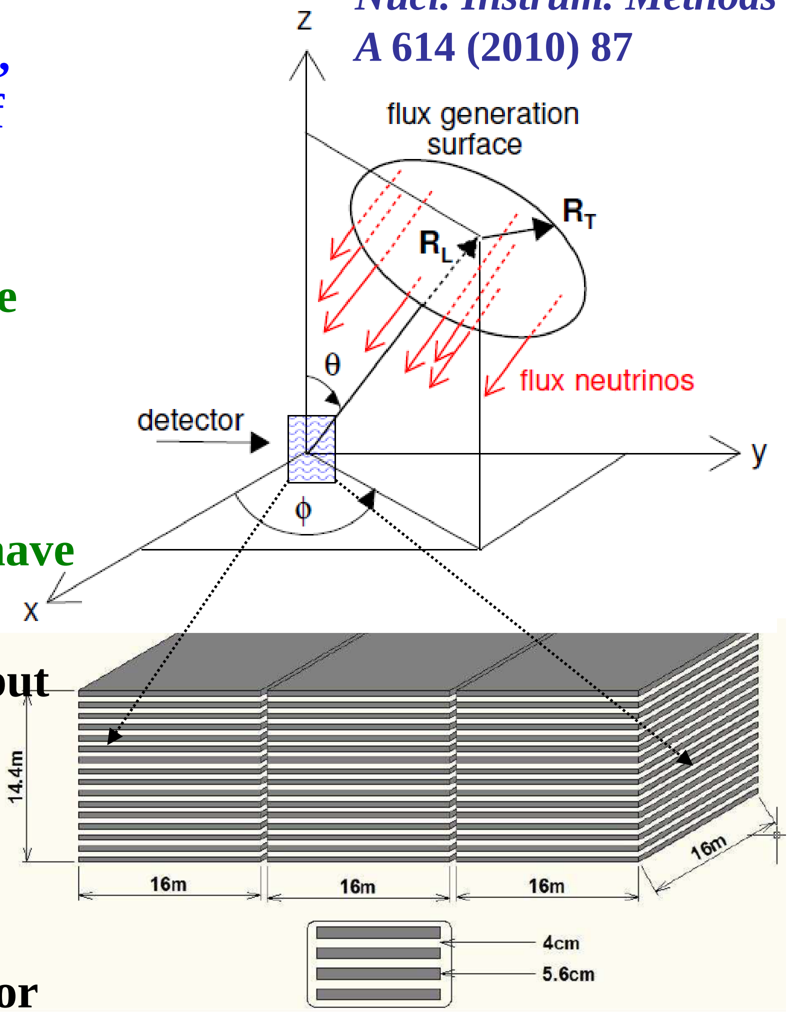

Details of detector material

(4) Take output in the root format to directly give as input to GEANT4 simulation

A word of Warning

- **[. . .] The Monte Carlo simulation has become the major means of visualization of not only detector performance but also of physics phenomena. So far so good. But it often happens that the physics simulations provided by the Monte Carlo generators carry the authority of data itself. They look like data and feel like data, and if one is not careful they are accepted as if they were data.**
- **[. . .] I am prepared to believe that the computer-literate generation (of which I am a little too old to be a member) is in principle no less competent and in fact benefits relative to us in the older generation by having these marvelous tools. They do allow one to look at, indeed visualize, the problems in new ways. But I also fear a kind of "terminal illness", perhaps traceable to the influence of television at an early age. There the way one learns is simply to passively stare into a screen and wait for the truth to be delivered. A number of physicists nowadays seem to do just this.**

J.D. Bjorken from a talk given at the 75th anniversary celebration of the Max-Planck Institute of Physics, Munich, Germany, December 10th, 1992. As quoted in: Beam Line, Winter 1992, Vol. 22, No. 4

This is even stronger in the use of machine learning from user point of view